Addis Ababa University
Addis Ababa Institute of Technology
School of Graduate Studies

School of Mechanical and Industrial Engineering

# Design and Analysis of Bumper for Three Wheeled Vehicle (Bajaj)

A Thesis Submitted to the School of Graduate Studies of Addis Ababa University in Partial Fulfillment of the Requirement of the Degree of Masters of Science in Mechanical Engineering

(Mechanical Design Stream)

By

Tewodros G/Michaiel

Advisor

Professor .Eyassu W/Senbet.

September, 27, 2017

Addis Ababa University
Addis Ababa Institute of Technology
School of Mechanical and Industrial Engineering

This is to certify that the thesis prepared by Tewodros G/Michaiel, entitled by Design and Analysis of Bumper for Three Wheeled Vehicle (Bajaj) that Assembled in Ethiopia and submitted in partial fulfillment of the required for the degree of Masters of Sciences (Mechanical and Industrial Engineering) complies with the regulation of the university and meets the accepted standards with to originality and quality.

Signed by the Examining committee:

Internal Examiner ____________________Signature ____________________Date _____________

External Examiner____________________Signature ____________________Date ____________

Advisor: ___________________________Signature _____________________ Date ____________

Co-Advisor:________________________ Signature _____________________Date____________

___________________________________________

School of Center Chair Person

## Acknowledgements

I would like to express my sincere and heartfelt gratitude to my advisor, Professor Eyassu Weldesenbet, for his guidance, constructive and stimulating comments and for his friendly treatment in all the consultation I had with him in this thesis work.

I would also like to thank my co-advisor, Mr.Mulugeta kahsay and other staff who provide me with valuable material, moral and information in conducting this study.

I am grateful to, Tagrow Bajaj industry Technical Manager, Ato Yonas and for the Ethiopian Traffic police bureau, for providing me with all information relevant to this research.

Besides, I would like to express my gratitude for the Department of Mechanical and Industrial engineering school, particularly for the design chair for facilitating my work. My deepest gratitude also goes to my friends who constantly provide me with support, encouragement and constructive ideas in the course this thesis work.

Finally, I would like to thank my loving family for their endless encouragement and support during the entire period.

## Abstract

This thesis aims for the design and analysis of bumper model using different geometrical shapes for optimizing a three wheeled vehicle (Bajaj) through addressing the factors that contribute to causalities and material losses sustained by the rising traffic accident. The study focuses on design the bumper model for absorbing kinetic energy during collision and sudden accident. Investigation of the most suitable and optimized geometrical design of three wheeled bumper at conceptual design stage is carried out using Computer-Aided Engineering. For this reason, the focus of the design is on increasing energy absorption at the moment of impact and on minimizing accidental failure of occupants and damage of the components of the vehicle.

Many researchers have identified that a three wheeled vehicle accident causes a catastrophic failure in human as well as vehicle. So, material selection and design parameter will minimize or reduce the occurrence of an accident.

This thesis demonstrates the deformation as well as the total energy absorption of the bumper model subjected to an impact velocity of different magnitude and geometry with a rigid wall for analysis. During the impact analysis maximum Von Misses stress, total deformation, internal energy absorption and specific energy absorption is also carried out by Ansys Explicit Dynamic Analysis for modeling and analysis of the complex bumper geometry for different geometrical shapes. The model was analyzed by explicit dynamic analysis using ANSYS Workbench 16.Among the two bumper model geometry (hexagonal and rectangular shapes), which are used for the explicit dynamic analysis, hexagonal geometrical bumper model possess lower Von-Misses stress value, highest internal energy, highest specific energy absorption and the lowest deformation, in view of rectangular geometry. This demonstrates that that the hexagonal geometry is better than rectangular bumper model.


**Key Words:** Explicit Dynamic analysis, specific Energy Absorption, Deformation, Hexagonal Geometry, Rectangular Geometry, impact

## Table of contents

## List of figures

## List of tables

## Nomenclature

CFRP: Carbon fiber reinforced polymer

FEM: Finite element method

NHTSA: National highway traffic safety administration

{F}: External force vector

{D}: Displacement vector

{σ}: Stress vector

{$\epsilon$}: Strain vector

COR: Coefficient of restitution

GF: Glass fiber

$E_{aa}$: Effective Young's modulus of the material in the aa-direction

$G_{aa}$: Effective shear modulus of the material in the aa-direction

$NU_{ab:}$ Poisson ratio interpreted as the free contraction of the material mid-plane in the b-direction in response to an imposed extension of the material mid-plane in the a-direction

$CTE_a$: Thermal expansion coefficient of the material in the aa-direction.

$+S_x$: Normal tensile strength of the material in the xx-direction.

$-S_x$: Normal compressive strength of the material in the xx-direction.

$S_{ab}$: Shear strength of the material in the ab-direction.

$+e_x$: Normal strain in the xx-direction caused by uniaxial tensile stress $+S_x$.

$-e_x$: Normal strain in the xx-direction caused by uniaxial compressive stress $–S_x$.

$E_{ab}$: Shear strain in the ab-direction caused by shear stress $S_{ab}$.

$K_x$: Thermal conductivity of the material in the xx-direction.

# Chapter 1

## 1.1. Background

### 1.1.1. Introduction

Three-wheelers, commonly known as Bajaj's, can be found all over the world, specifically in Asia. And they are used for transporting persons or freight. In Ethiopia, three-wheeler vehicles are used in transportation sector particularly in cities of regional states, among others, Dire Dawa, Harar, Jijiga, Bahir Dar, Hawassa, Adama and Mekele. Most of the three-wheelers in Ethiopia are imported from India. These vehicles are providing transport services, mainly for public transport, and at a time for goods. In state cities in Ethiopia, they are becoming more and more common in the transportation sector. Nowadays, research findings show that the causalities and injuries sustained by pedestrians, occupants and material damages as a result of crashes of three wheeled vehicles are becoming serious from time to time.

The increase in traffic accident attracted the attention of researchers, focused on the safety characteristics of three wheeled vehicles. Different scientific studies on road traffic crashes and possible solution will result mainly from design parameters and safe driving. As a result, a major proportion of the safety research effort has focused on the problems of the three wheeled vehicle occupant and component of the vehicle.

The best internal safety and bumper design protect the vehicle and occupants from serious damage; and they minimize the expense of repair parts. The study will focus on design for absorbing kinetic energy during the collision and sudden accident. The study also aimed for investigate the most suitable optimized design of three wheeled bumpers using Computer-Aided Engineering.

In addition to mechanical property of the bumper material, the designed bumper increasing and improvement of performance are evident compared to the current safety systems. The major outcomes expected which from this thesis are to increase the energy absorption of the bumper model during the crash and at the same time to minimize the injuries that the occupants suffer.

Moreover, the bumper of the three wheeled vehicle is subjected to dynamic and impact loads which could be detrimental by the strength and rigidity of the overall structure. That is why the frame structure is designed to withstand static and dynamic service loads encountered during the vehicle's life cycle. In addition, the vehicle structure is designed to maintain its integrity and provide an adequate protection for most accident. The crashworthiness of the vehicle is an important security measures, and improves the impact safety performance of a vehicle.

### 1.1. 2.Energy absorption

Most vehicle energy absorbers in the market today are designed to meet safety regulations with respect to specific geographic locations. However, the designing of bumper system that is rigid enough to protect the vehicle and, at the same time, the pedestrian is much more difficult.

There are two types of energy absorbers widely used in the automotive industry. The shock absorber type, also known as the hydraulic design, is a telescopic energy absorbing cylinder mounted between the front bumper and the front cross member of the chassis. On the other hand, the honeycomb type also known as the cell block deformation design has collapsible cells embedded in the bumper structure. The shock energy absorber is a link member between a bumper and a front cross member for the purpose of damping the loading during a low-speed collision between the vehicle and an obstacle.

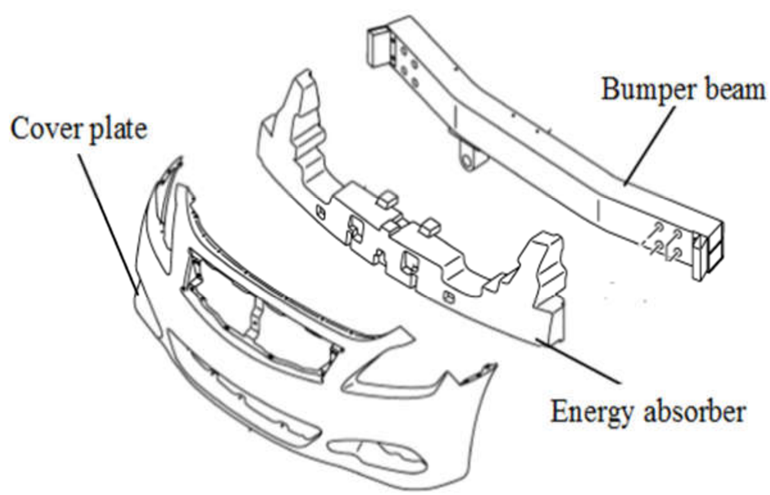


Figure 1.Components of bumper (Muhammad S., Hambali A., Rosidah , Widodo W.S and Ahmad M.N, 2017)

The intended function of bumper components is to absorb kinetic energy during the vehicle collision. The energy absorbers are generally made of different material and compositions. This study is also considers different reinforcement materials so as to withstand the impact of the crash, that which causes serious damage.

The bumper is one of the most important automotive parts in crash energy absorption. In the case of a crash accident, a bumper is expected to be collapsed with absorbing crash energy prior to the other body parts so that the damage to the main body frame is minimized and passengers are saved. Energy generated from the collision of vehicle has been absorbed mainly by the plastic deformation of the absorber material. To ensure that the crash box absorbs the entire energy in the collision, it requires the impact velocity, which is evenly distributed to protect other structures damage, and all the kinetic energy was absorbed.

### 1.1.3. Types of Bumpers

#### 1.1.3.1. Carbon Fiber Bumpers

Carbon fiber reinforced polymer is an extremely strong and light which contains carbon fibers. Polymers that are usually used for binding are mainly thermo set resins. Epoxy is one of the thermo set resin and other resins are also used for binding purpose, such as polyester, vinyl ester or nylon. The required strength of the carbon fiber reinforced polymer is obtained from reinforcement through measuring the stress and elastic modulus of the reinforcement composite. Unlike isotropic materials like steel and aluminum, CFRP has directional properties. CFRPs demonstrate excellent corrosion resistance; and the effect of moisture at wide ranges of temperatures can lead to the degradation of the mechanical properties of CFRP, particularly at the matrix–fiber interface. Carbon Fiber bumper are light weight bumpers as compared to conventional bumpers made of steels. Carbon fiber body work is normally the thing of super-cars, but many a car companies and specialist modifiers, are starting to use it for replacement body parts on everyday cars. [10]

#### 1.1.3.2. Aluminum Honeycomb Sandwich Panel Bumpers

The geometry of a honeycomb minimizes the amount of material used. So, it minimizes costs and weight. This aluminum honeycomb is produced by the expansion process. This type of construction consists of thin two facing layers separated by a core material. The aluminum honeycomb panel provides light weight, high rigidity and high structural stability. [10]

#### 1.1.3.3. Steel Bumpers

Steel front bumper are mostly used in off road vehicles which have a coating to influence the corrosion life of the bumper. Steel is often e-coated and then painted or powder-coated. Steel bumpers are made of bare steel and are then e-coated after the forming process. Some steels are coated with zinc which improves the life of the steel by discouraging or preventing corrosion. In past, steel bumpers were very thick due to which it increases the weight. [10]

#### 1.1.3.4. Plastic bumper

The modern cars use a reinforced thermoplastic bumper, as they are cheap to manufacture, easy to fit and absorb more energy during a crash. A majority of car bumpers are custom made for a specific model, so if you are looking to replace a cracked bumper with a similar one, you would have to buy from a specialist dealer. However, many companies now offer alternative designs in thermoplastic, with a range of fittings designed for different models.[11]

#### 1.1.3.5. Metal Foam Bumpers

The metal foam has a cellular structure which consists of a solid metal as well as it has a pore which makes it an ultra-light material. The aluminum and its alloys have a low density which it is used as metal foam. Bumpers made of metal foam, possess high compression strength. Generally, there are two types of metal foam open and close type. Bumpers, which automotive industry manufacturers, are mostly closed type. This is because they provide optimal energy absorption. Many automakers uses aluminum foam crash box which is placed between impact beam and front rail of car. During collision, at slow speed of about 15km/hr, they deform and absorb all energy. As a result protecting all valuable parts at the front end and the car frame will be protected. [10]

### 1.1.4. Composite material overview

Composite materials are composed of matrix and a reinforcement structure which give desirable properties rather than the individual constituent. Fiber reinforced polymer matrix composites are hugely used composites. Glass fiber, carbon fiber and boron fiber are the most common types of fibers used in composites in terms of strength and cost consideration. [15]

Composite materials have numerous advantages over more conventional materials because of their superior specific properties; such as high strength and stiffness to weight ratio, improved corrosion, and environmental resistance as well as, design flexibility, improved fatigue life, and potential reduction of processing, fabrication and life cycle cost .[16]

#### 1.1.4.1. Epoxy Resins

Epoxy resins represent the highest performance resins of those available at this time. [17] For a composite material, epoxy material is highly used. Epoxy has extremely good properties and it acts as very good adhesive, it has high strength, low shrinkage and it is a very fine anti corrosive material. [15]They have generally more effective performance in binding process than other resin types in terms of mechanical properties and resistance to environmental degradation, making them almost for exclusive use in aircraft technology components. As a laminating resin their increased adhesive properties and resistance to water degradation make them ideal for use in applications such as boat technology. So epoxies are widely used as a primary construction material for high-performance. [17]

#### 1.1.4.2. Fibers

Glass fiber is among the most versatile industrial materials known today as E-Glass fiber. And they are available in unlimited supplies. E-Glass fibers exhibit useful bulk properties such as hardness, resistance to chemical attack, stability, strength, flexibility, and stiffness. They are used in the manufacture of structural composites and special-purpose products. [18]

Glass fibers are categorized as, low-cost general-purpose and premium special-purpose fibers. Over 90% of all glass fibers are general-purpose products. These fibers are known by their designation as E-glass while the remaining glass fibers are premium special-purpose products. [19, 20]

## 1.2. Statement of the Problem

Nowadays traffic accident rate of three wheeled vehicle is becoming higher and higher .Hence, vehicle safety is an important research area to protect the occupants as well as the structure during an impact. So to alleviate traffic accident, injuries, causalities and damage of vehicle component, developing the best energy absorber bumper model, employing suitable bumper geometry design is a necessary for improving the toughness and protecting the vehicle structure as well as minimizing the severity of human injuries.

## 1.3. Objective

### 1.3.1. General objective

The major objective of this paper is to design of best energy absorber bumper through different geometry for a three wheeled vehicle (Bajaj) that assembled in Ethiopia using FEM & ANSYS.

### 1.3.2. Specific Objective

The specific objectives are:

- ✓ Develop bumper model using solid work software.
- ✓ Analyze the stress concentration on the model by using Ansys software.
- ✓ Analyze the effect of impact velocity on the model using Ansys software.
- ✓ Analyze the effect of different loading condition on the model.
- ✓ Identify the critical point or maximum area of the stress distribution.
- ✓ Identify the deformation of the model due to the applied velocity
- ✓ Compare the models result with each other.

## 1.4. Scope of the Study

Basically three wheeler vehicles (Bajaj's) are found all over the country and they have played a significant role in providing transportation services for peoples and goods. Though, assessment of entire vehicle accidents occurred in human lives and on property in country would make comprehensive study and sound findings, this thesis is limited only to three wheeler vehicles (Bajaj's).So this thesis aim for reducing injury rate in human lives and material losses which result from Bajaj accident through employing the best and suitable energy absorber bumper design model.

## 1.4. Organization of the Thesis

The thesis is organized in to six chapters. In the first chapter, background and introduction of the thesis, objectives to be achieved, scope of the study and organization of the paper discussed. In the second chapter, related literature review and thesis work are reviewed to research how different researchers have carried out their research what material, method and experiment they used. The third chapter discusses about methodology of the study based on analytical method of bumper components in related to energy absorption rate and crashworthiness analysis regarding the solid geometric model in accordance with the boundary condition that meet the energy absorption. In the fourth chapter, finite element method (FEM) is used, mainly, Ansys to develop crash analysis, and 3D finite element analysis is carried out using Ansys software to give a detailed analysis during an impact. In the fifth chapter, analysis results are summarized and discussions are made based on the FEM and Ansys analysis results. Finally, it gives a comparison based on the model solutions that is done. The sixth chapter provides the conclusion based on the analysis results and suggests future work.

# Chapter 2

## 2.1. Literature review

Reviewing of the existing literature provide better insight for creating a better design and reduction of injury in three wheelers vehicle (Bajaj's) during accident in Ethiopia . Different researches were done on different bumper analysis in different material, method and experiment in the world in terms of cost effective and reasonable for uses. This is done by using different approaches;

### 2.1.1. Literature review according to methods

According to Prabhakaran , Chinnarasu and Senthil Kumar they follows national highway traffic safety administration (NHTSA) produces some bumper standard for light passenger vehicle to know the performance requirements for passenger cars in low-speed front and rear collisions. It applies to front and rear bumpers on passenger cars to prevent the damage to the car body and safety related equipment. The all bumper should satisfy the following bumper standards,

- ✓ The front and rear bumpers on passenger cars should prevent the damage to the car body.
- ✓ The bumper withstand at a speed of 2 mph across the full width and 1 mph on the corners.
- ✓ Bumper should also withstand 5 mph crash into a parked vehicle.
- ✓ Placement of the bumper is 16 to 20 inches above the road surface.[9]

The design of the composite bumper is by using the existing ambassador steel mould. They take the dimensions steel bumper. [9] Thus are

- ✓ Effective length
- ✓ Total length
- ✓ Thickness
- ✓ Effective breath
- ✓ Total breath
- ✓ Weight
- ✓ Material
- ✓ Tensile strength
- ✓ Density

They apply theory of bending [9] and also Newton second law of motion to determine the force acting on the bumper.

Pandey, Patil and Nikumbh shows in their comparative study they shows that the selection of bumper material is very important for safety of an automotive part and also safety of pedestrian during low speed collision. They study the properties of different bumpers and compared with carbon fiber reinforced plastics bumper, finally they deduced those carbon fiber reinforced plastics bumpers are very light in weight than the other bumpers. From the result of their studies steel bumpers are the heaviest and thickest bumper compared to other bumper. [10]

Pandey, Patil and Nikumbh shows in their comparative study they shows that an aluminum honeycomb sandwich structures are light weight and gives an advantage on saving money in terms of fuels and to get optimum speed much quicker with less efforts. Metal foam bumper are ultra-light in weight because of the structure have a percentage of 70% - 90% of the volume consists of a void spaces. [10]

Pandey, Patil and Nikumbh shows in their study honeycomb structure also has a cell geometry which is capable of elastic buckling, which gives the honeycomb structure to recover their shape and properties after collision. Aluminum honeycomb structure if deformed in collision then they have to be changed or repaired. The honeycomb structure has strength and absorbs more energy which insures passenger safety. [10]

Tekavde , Srinivas , Banthia , and Mittemari states that the general vehicle structure to provide safe structural environment for occupants of vehicles involved in high speed (> 15 km/h) collisions has drawn considerable resources as safety of humans is at stake. Low speed impacts, since these do not cause severe injuries to the occupants, do not generate much concern. However, structural design for this situation has generated a lot damage caused by these types of collisions. Various designs of crash-box that can be fitted within the packaging space have been assessed for low speed impact. Geometric parameters like length, wall thickness, cross-section shapes (rectangle, hexagon and octagon). Through use of thinner walls it was possible to limit major deformation to the crash-box. The major use of the crash-box is to reduce a permanent deformation and to decrease the replacement of rails after impact. [1]

Liu, Ding, Yan, and Yang Yong**,** states that Crash box produced axial deformation; performance of collision reflected the mechanical properties of the relationship between the force and displacement. The crashworthiness evaluation parameter including the absorption of the total energy E**,** the peak impact force $F_p$ , compressed displacement of crash box $\delta_e$ and the average impact force $F_m$**.**

1. Absorption of the total energy E

Crash box absorbed total energy by the equation

$$E = \int_0^{\delta} F(s)ds$$

Where: F(s) - Impact force and s- Deformation

2. The peak impact force $F_p$

The peak impact force $F_p$ related with cross-section shape and materials of crash box, design of crash box according to stiffness of link vehicles to identify impact force license value, the peak impact force cannot exceed the license value, otherwise vehicles other parts will be damaged.

3. Compressed displacement of crash box $\delta_e$

In low-speed frontal crash, the collision kinetic energy was basically absorbed, the smaller the compression displacement of crash box, the more the remaining space.

4. The average impact force $F_m$

The average impact force shown as

$$F_m = \frac{E}{\delta_e}$$

Where： E - Absorption of energy

$\delta_e$ - Compressed displacement of crash box

$F_m$ is arithmetic average value, with $F_m$ increasing, the absorbing energy of crash box will increase. As crash box is determined by the length, the greater the average impact of crash box is, the more energy absorb, the better the safety crew are protected. Therefore, the bigger average impact force is, the better the absorption performance. [2]

A. Siva, G.Himabindu, M.Sankar and K.Vijaya they enables geometric design of the longitudinal members, and first be cleared that what kind of loads can occur in real frontal collisions. These loads are determined by the parameters describing the frontal crash and their predominant values. Besides the collision speed, the obstacle type, the impact location and direction, also the vehicle mass has a large influence on the crash behavior. [3]

Qing-fen, Hai-dou, Yan-jie, Sheng-yuan they states that crash-box is one of the most important automotive parts for crash energy absorption. In case of frontal crash accident, it is expected to be collapsed with absorbing crash energy prior to other body parts so that the damage of the main cabin frame is minimized and passengers may be saved. They study the energy absorption characters of automobile crash-box at low-velocity impact by using Finite Element Method and shape optimization design for thin-walled tubes and proposed a cross section and adopting appropriate grooves. The results show that the energy absorption characters improved obviously for square cross section thin-walled tube with double concave and bulgy grooves. [4]

### 2.1.2. Literature review according to material

According to Prabhakaran, Chinnarasu and Senthil Kumar they design, fabrication and testing of steel and composite bumper. They also compared the result of the two bumpers in related to weight, fuel economy, and cost and impact resistance. As a result for the same model of the bumper give a steel bumper weighs 5.15Kg and the weight of composite bumper is 2.38kg. This shows that the percentage ratio of 53.8% lesser than steel bumper as the result fuel economy of the vehicle is improved. Cost of composite bumper is 80% less than steel bumper so composite materials are cost effective than the steel material. [9]

Pandey, Patil and Nikumbh shows in their study honeycomb structure also has a cell geometry which is capable of elastic buckling, which gives the honeycomb structure to recover their shape and properties after collision. Aluminum honeycomb structure if deformed in collision then they have to be changed or repaired. Actually most of the bumpers have to be changed or repaired if possible after its first collision. CFRP is the costliest one because of its long and arduous manufacturing process. The honeycomb structure has strength and absorbs more energy which insures passenger safety. Foam bumper made by Age-hardening of aluminum shows the improvement of foam with large void sizes but not with small sizes. Mostly steel bumpers are used in heavy vehicles and rests of the bumpers are used in almost all types of vehicles. [10]

M. Anil Kumar and N. Phani Raja Rao they analysis a bumper modeled at different speeds for different materials Steel, ABS Plastic and Carbon Fiber-Reinforced. Carbon reinforced have less than that of steel that means the stress values are less and comparing the results, the stress values are less for composite. Then finally they suggested that composite materials are best for car bumper than steel. [11]

Mr. Vishal S. Jagadale and Prof. Laukik B. Raut they deal in the experimental investigation of mechanical properties of glass fiber/epoxy composite material with variation in volume fraction of fiber in the composites. For manufacturing of composites combined hand layup and compression molding methods are used. The volume fraction of fiber is maintained about 40%, 50% & 60% in the total composition. With the help of experimental testing the mechanical properties such as tensile strength, shear strength. The results shows better mechanical properties with 50% of Volume fraction, however further increase in fiber content increases mechanical properties but composites starts delaminating. So at the end they got the mechanical property of the material with 50:50 compositions. And they suggested that 50:50 composition ratio is better for application with optimum strength. [5] The fiber orientations enhance the energy absorption capability of the composite material. The type of reinforcing fiber used in a composite material determines to a very large extent its energy absorption characteristics. [7]

### 2.1.3. Literature review according to experiment

According to Prabhakaran, Chinnarasu and Senthil Kumar they design, fabrication and testing of steel and composite bumper through the experimental result they deduce that the Impact strength of composite bumper is 7.35 J/mm$^2$ where steel bumper is 3.25 J/mm$^{\mathbf{2}}$. And also by using ANSYS software they analyzed steel and composite bumper model to determine maximum stress induced in the composite bumper and get a numerical value for composite is 159.36 N/mm$^{\mathbf{2}}$ but in steel is 292.669 N/mm$^{\mathbf{2}}$ and the factor of safety for composite bumper is increased by 64%. They concluded that fiber reinforced plastic material is best material for bumper. [9]

According to Prabhakaran, Chinnarasu and Senthil Kumar they use charpy impact testing to measure a material’s ability for an impact resist to determining factor in the service life of the material.  They use the test to determine the amount of energy absorbed by a material during fracture because the absorbed energy gives material’s toughness. They take a specimen with a  dimensions are v-shaped notch, 2mm deep, with 45$^0$ angle and 0.25mm radius along the base. They used Ansys software for static-nonlinear analysis to determine the deformation, stress distribution over the structure. Using

ANSYS software they analyzed steel and composite bumper model and determine maximum stress induced in the composite bumper and steel. [9]

M. Anil Kumar and N. Phani Raja Rao they study a 3D car bumper modeled using modeling software Pro/Engineer and apply an impact analysis on the bumper at different speeds of 48Km/hr, 75Km/hr and 150Km/hr. [11]

In Mr. Vishal S. Jagadale and Prof. Laukik B. Raut study on a composite material made up of glass fiber and epoxy resin with different volume fraction. through choosing an appropriate mixture of matrix and reinforcement or fiber material, a new material can be made that exactly meets the requirements of a particular application. The composite material has an orthographic property, which means different property in all directions. For experimental they take Epoxy resin and Epoxy hardener and they were mixed in the ratio of 10:1 by the weight. And also for experiment they take E- Glass fiber with composition. Finally apply the Fabrication of FRP composite in three types with different volume fraction using hand lay-up method. Their respective volume fraction is 40:60, 50:50 and 60:40 with lamina size of 300×300×3mm. The lamina specimen is prepared according to the ASTM D732-2010 standard. Then apply tensile and shear test for the lamina. Finally they conclude that an increase in fiber content increases mechanical properties but increases brittleness and start delaminating. The material with 50:50 compositions is good for application as it has optimum properties with less brittleness. [5]

# Chapter 3

## 3.1. Research Methodology

### 3.1.1. Introduction

The research focuses on the minimization of damage on the Bajaj component as well as humans during Bajaj accident that assembled in Ethiopia using suitable bumper geometry model. For such an accident the best way of minimizing the injuries of an accident, bumper design is the best alternative than the other Bajaj's body parts in terms of economy. Honeycomb Bumper is a cost effective way of developing an impact absorbing bumper that is light in weight, high in strength and stiff in low-speed collision but the cells are not retractable or do not move back into position.

The data collection has been done from local assembling company manuals and modeling of the bumper by using Ansys from the existing Bajaj model specification. Then the Finite element analysis using Ansys explicit dynamic has been performed for different bumper model.

### 3.1. 2. Methodology of the research

Some methods that will be used in order to fulfill the basic objective of the Bajaj bumper design analysis for impact resistance are:

- ❖ Data collection of the Bajaj through surveying and documentation
- ❖ Identifying the composite material for absorbing impact energy
- ❖ Mathematical modeling of the Bajaj structure for geometrical analysis
- ❖ Selecting appropriate geometric and model the bumper using Ansys software.
- ❖ Stress analysis of the model using Ansys software under operating condition
- ❖ Identifying the equivalent design parameters and stress for the bumper materials under different loading conditions
- ❖ Discussing the similarity and difference of the bumpers structure for different geometry

The above methods are applied at a specified conditions and constraints with appropriate methodologies to achieve the most suitable and reliable result.

### 3.1.3. Conceptual Framework

The conceptual framework shows a method followed in the overall analysis and improvement of the Bajaj bumper based on loading conditions and energy absorption rate until reasonable result can be shown in the new model.

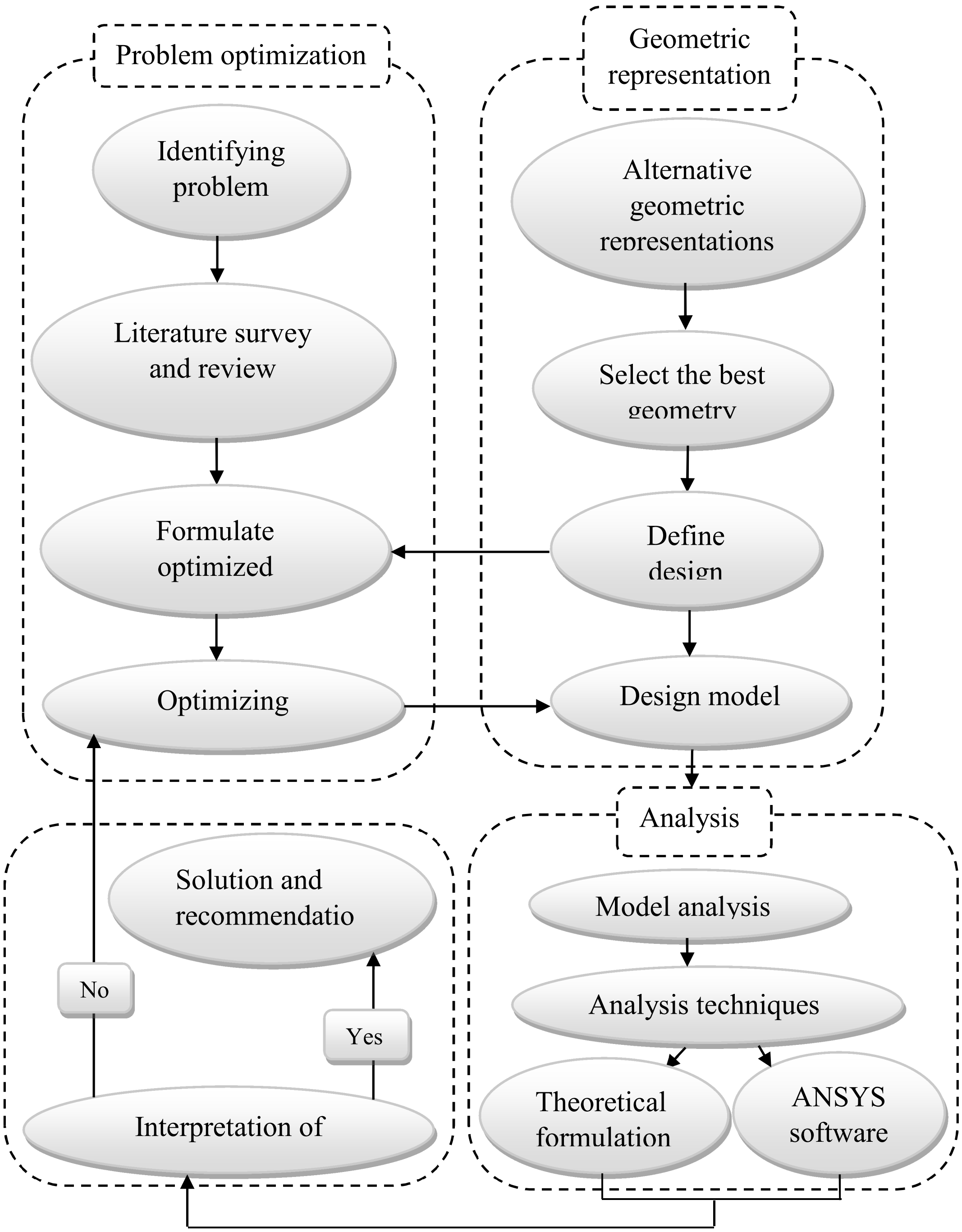


Figure 3. 1.Conceptual framework

## 3.4. Finite Element Analysis

The finite element method (FEM) is a simplified approximate solution for many engineering systems through subdividing them into components or elements. The system response analysis is described by the complex differential equation that means the response with a number of unknowns. The model can be represented by an equation; it can be analyzed by employing a finite number of components and simple matrices. The system accuracy of the solution can be controlled by changing the number of unknowns and elements numbers. The steps in the analysis the systems are as follows:

- ✓ Geometry of the model: The geometry of the model shown by its elements and nodes.
- ✓ Material definitions, which are usually associated with parts of the geometry.
- ✓ Parts and an assembly: the geometry can be divided into parts, which are positioned relative to one another in an assembly.
- ✓ Initial conditions: non-zero initial conditions such as initial stresses, temperatures or velocities can be specified.
- ✓ Boundary conditions: zero-valued boundary conditions (including symmetry conditions) can be imposed on the model.
- ✓ Constraints: linear constraint equations or multi-point constraints can be defined.
- ✓ Contact interactions: contact conditions between surfaces or parts can be defined.
- ✓ Output control: options for controlling model definition output to the data file
- ✓ Analysis continuation: it is possible to write restart data or to use the results from a previous analysis and continue the analysis with new model or history data

The finite difference is a well-established and conceptually simple method that requires a point-wise approximation to the governing equations. The model, formed by writing the difference equations for an array of grid points, can be improved by increasing the number of points. Although problems solved by using the finite difference methods for different geometries of boundary conditions through difference technique.

## 3.5. Nonlinear Finite Element Modeling

Contact by nature is a nonlinear boundary value problem. During contact (impact), both the forces transmitted across the surface and the area of contact change this give the contact stress is transmitted in the normal direction. But if the friction is present at the contact area, shear stress is also transmitted. Therefore During crash (impact), the three wheeled vehicles (Bajaj) parts experience high impact loads resulting in high stresses. These stresses approach material yield load or buckling critical limit the structural components experiences large progressive elastic-plastic deformation or buckling. So in nonlinear finite element method analytical solutions are becoming the suitable approach to minimize such problem through different package software. The mathematical basis of the nonlinear finite element method is discussed as:

### 3.5.1. Basic Governing Equations

The Principle of Virtual Work establishes a relation between variations in internal and external work due to infinitesimal displacement variations for a deformable body. Virtual work is the work done by the real force acting through a virtual displacement or a virtual force acting through a real displacement. A virtual displacement is any displacement consistent with the constraints of the structure, i.e., that satisfy the boundary conditions at the supports. A virtual force is any system of forces in equilibrium. The structure deformed by the effect of n external forces, denoted by the vector {F} and the actual (real) displacements at the same n coordinates are contained in the vector {D}. Therefore the stresses and strains at any point in the structure are elements of the vectors {σ} and $\{\epsilon\}$:

$$\{\sigma\}^{T} = \{\sigma_{xx} \quad \sigma_{yy} \quad \sigma_{zz} \quad \tau_{xy} \quad \tau_{xz} \quad \tau_{yz}\}$$

$$\{\epsilon\}^{T} = \{\epsilon_{xx} \quad \epsilon_{yy} \quad \epsilon_{zz} \quad \gamma_{xy} \quad \gamma_{xz} \quad \gamma_{yz}\}$$

The total external work done by {F} is

$$w = \frac{1}{2}\sum_{i=1}^{n} F_i D_i = \frac{1}{2}\{F\}^{T}\{D\} \quad \text{......(1)}$$

And the total internal work done by {F } is the total strain energy, which can be written as

$$U = \frac{1}{2}\int \{\sigma\}^{T}\{\epsilon\}\, dV \quad \text{......(2)}$$

This gives ***w*** equal to **u** gives the principle of real work

$$\frac{1}{2}\{F\}^{T}\{D\} = \frac{1}{2}\int \{\sigma\}^{T}\{\epsilon\}\, dV \quad \text{...... (3)}$$

After the structure is subjected to the system of n external forces {F}, producing internal stresses {σ}, a system of m virtual forces {F}' are applied, producing additional virtual deformations {D}', virtual stresses {σ}' and virtual strains $\{\epsilon\}'$

The external work done by the application of {F}' is

$$w = \frac{1}{2}\sum_{j=1}^{m} \mathrm{F}_j' \, \mathrm{D}_j' + \frac{1}{2}\{F\}'^{\mathrm{T}}\{D'\} = \frac{1}{2}\{\mathrm{F}\}'^{\mathrm{T}}\{D\}' + \{\mathrm{F}\}^{\mathrm{T}}\{D\}' \quad \ldots\ldots\ldots\ldots (4)$$

and the internal work done by the application of {F}' is

$$U = \frac{1}{2}\int\{\sigma'\}^{\mathrm{T}}\{\epsilon'\}\,dV + \int\{\sigma\}^{\mathrm{T}}\{\epsilon'\}\,dV \quad \ldots\ldots\ldots\ldots (5)$$

Then equating the above two equations of internal and external work at equilibrium

$$\frac{1}{2}\int\{\sigma'\}^{\mathrm{T}}\{\epsilon'\}\,dV + \int\{\sigma\}^{\mathrm{T}}\{\epsilon'\}\,dV = \frac{1}{2}\{\mathrm{F}\}'^{\mathrm{T}}\{D\}' + \{\mathrm{F}\}^{\mathrm{T}}\{D\}' \quad \ldots\ldots\ldots\ldots (6)$$

But when we consider the system as virtual system alone, then the external work and internal work is given as respectively.

$$w = \frac{1}{2}\{F\}'^{\mathrm{T}}\{D'\} \quad \ldots\ldots\ldots\ldots (7)$$

$$U = \frac{1}{2}\int\{\sigma'\}^{\mathrm{T}}\{\epsilon'\}\,dV \quad \ldots\ldots\ldots\ldots (8)$$

The applying equilibrium to the virtual system

$$\frac{1}{2}\int\{\sigma'\}^{\mathrm{T}}\{\epsilon'\}\,dV = \frac{1}{2}\{F\}'^{\mathrm{T}}\{D'\} \quad \ldots\ldots\ldots\ldots (9)$$

Then substituting equation (9) in to (6) then we get

$$\int\{\sigma\}^{\mathrm{T}}\{\epsilon'\}\,dV = \{\mathrm{F}\}^{\mathrm{T}}\{D\}' \quad \ldots\ldots\ldots\ldots (10)$$

Before applying the actual loads {F} and deformations {D} the structure is subjected to a of m virtual forces {F}'. And producing internal stresses {σ '}.Then the equilibrium equation became

$$\int\{\sigma'\}^{\mathrm{T}}\{\epsilon\}\,dV = \{\mathrm{F}\}'^{\mathrm{T}}\{\mathrm{D}\} \quad \ldots\ldots\ldots\ldots (11)$$

The above equation is used to find redundant forces (reactions) and real structural displacements shown for a short period of time interval. Equation (11) is applicable for linear and nonlinear elastic structures.

### 3.5.2. Direct Integration Methods

Implicit and Explicit are two types of approach that can be used to solve the finite element problem. The implicit approach is useful in problems in which time dependency of the solution is not an important factor [e.g. static structural, harmonic, modal analysis etc.] whereas Explicit Dynamics approach is most helpful in solving high deformation time dependent problems such as Crash, Blast, Impact etc.

The prime difference between the implicit and explicit scheme lies in the consideration of velocity or acceleration. We must aware of the equation relating mass (m), damping (c), stiffness (k) and force (F). In equation (12),' x' stand for displacement whereas $x'$ and $x''$ are stand for velocity and acceleration respectively. The transient nonlinear dynamics uses both implicit and explicit direct integration methods for solving the equations of motion,

$$m\,x'' + c\,x' + kx = F \quad \ldots\ldots (12)$$

$$[m]\,\{x\}'' + [c]\,\{x\}' + [k]\{x\} = \{F\} \quad \ldots\ldots (13)$$

But the choice of whether to use an implicit or explicit method is depends on:

- ✓ Nature of the dynamic problem
- ✓ Finite elements model

There are two methods to solve Equation. (13), implicit method and explicit method resp.

3.5.2.1. Implicit Method

In an implicit method, the nonlinear matrix equations of motion are solved at each time step to advance the solution. Treatment of boundary nonlinearities must occur within a time step. Large time steps may be used in implicit dynamic analysis. In an implicit scheme, the displacement is not a function of time (i.e. x = constant). Hence the velocities and accelerations which are time derivatives of displacement turn out to be zero and the mass and damping factors can be neglected. In order to solve an FEM problem using implicit method, inversion of stiffness matrix (k) is required. Implicit method mainly used in software such as Ansys, Nastran, Abaqus etc.

$$[m]\{x\}'' + [c]\{x\}' + [k]\{x\} = \{F\} \quad (14)$$

$$[k]\{x\} = \{F\} \quad (15)$$

The implicit method requires time derivatives of the displacement.

### 3.5.2.2. Explicit Method

Explicit methods are conditionally stable for undamped linear systems. For a given time step, an explicit operator requires fewer computations per time step than an implicit one. Explicit is a function of time, velocity and acceleration as well as the mass and damping need to be considered. In an explicit method, Central Difference time integration (CDTI) is used to calculate field variables at respective nodal points. Since only a numerical solution is possible for a nonlinear ordinary differential equation, this method is particularly suited for nonlinear problems. It requires the inversion of the lumped mass matrix as opposed to that of the global stiffness matrix in the implicit methods.

$$[m]\{x\}'' + [c]\{x\}' + [k]\{x\} = \{F\} \quad (16)$$

The explicit method is suitable for nonlinear transient dynamic analysis problems with very short durations of time intervals such as crash analysis problems.

#### 3.5.2.2.1. Central Difference Method

The central difference method one type of explicit method that approximates acceleration and velocity at time t + Δ t. The equation of the motion for the body is integrated using a central-difference integration rule:

$$x'^{N}_{\left(i+\frac{1}{2}\right)} = x'^{N}_{\left(i-\frac{1}{2}\right)} + \frac{\Delta t_{(i+1)} + \Delta t_{(i)}}{2}\, x''^{N}_{(i)} \quad (17)$$

$$x^{N}_{(i+1)} = x^{N}_{(i)} + \Delta t_{(i+1)}\, x'^{N}_{\left(i+\frac{1}{2}\right)} \quad (18)$$

Where $x^N$ refers to the degree of freedom (Displacement/Rotation) number N, subscript i refer to the increment number, Δ t is the time-step. x' and x'' are velocity and accelerations of the previous time step. The efficiency of the explicit time-step originates from the use of diagonal (lumped) element mass matrices since the accelerations at the beginning of the increment are calculated by

$$x''^{N}_{(i)} = (M^{NJ})^{-1} (P^{J}_{(i)} - I^{J}_{(i)}) \quad (19)$$

Where $M^{NJ}$ is the lumped mass matrix, $P^{J}$ is the applied load vector, and $I^{J}$ is the internal force vector. The diagonal mass matrix can be simply inverted. Other reason for added computational efficiency of the method is the fact that the tangent stiffness matrix is not needed and no iteration need to be performed during analysis. The internal force vector is assembled by element contributions.

### 3.5.3. Impact Theory

The two basic types of impacts are elastic impact and plastic impact. In an elastic impact some of the energy can be lost between the two impacting objects, while in a plastic impact the energy dissipated in the collision. An impact between two bodies is characterized by the presence of forces of large magnitude and short time duration. Because of these forces sudden changes occur in the velocities of the bodies, and it is these velocity changes which are ordinarily observed and gives impact result. If the forces acting on the bodies were known, the solution of an 'impact problem would require only the integration of the equation of motion. The motion of the bodies during impact must always satisfy the momentum equation, the energy equation, and the third law of motion. These are sufficient to determine all motion except those occurring during the time of impact. Two bodies colliding with velocities $u_1$ and $u_2$ **,** the location and direction of the forces can be determined from the geometry of the impact bodies, and hence the locations and directions of the impulses $I_1$ and $I_2$ acting on the body are known. The impulses are equal and opposite:

$$I_1 = - I_1 = I \quad (20)$$

And the impulse-momentum relations for the impact bodies

$$m_1( v_1 - u_1) = I \quad (21)$$

$$m_2( v_2 - u_2) = -I \quad (22)$$


Figure 3. 2.Vehicle impact with different velocity

Where: $v_1$ and $v_2$ are the velocities after impact.

The additional equation that is required can be obtained from energy considerations. For the impact of perfectly elastic with no energy loss, then the equation of the conservation of energy

$$\frac{1}{2}m_1u_1^2 + \frac{1}{2}m_2u_2^2 = \frac{1}{2}m_1v_1^2 + \frac{1}{2}m_2v_2^2 \quad \text{……………………………..…. (23)}$$

If the impact forces are large to produce permanent deformations of the bodies, the work done that makes a deformations represents an energy loss which may be too large to be neglected. In case of collision the impact for which the changes in velocities are parallel to the x-axis. The energy and momentum equations for no energy loss written as:

$$\frac{1}{2}m_1x'^2_1 + \frac{1}{2}m_2x'^2_2 - E = \frac{1}{2}m_1X'^2_1 + \frac{1}{2}m_2X'^2_2 \quad \text{………………….…… (24)}$$

$$\frac{1}{2}m_1(x'_1 - X'_1)(x'_1 + X'_1) = -\frac{1}{2}m_2(x'_2 - X'_2)(x'_2 + X'_2) \text{….. (25)}$$

$$\frac{1}{2}m_1(x'_1 - X'_1) = -\frac{1}{2}m_2(x'_2 - X'_2) \text{…………………………….... (26)}$$

Dividing the first equation by the second gives:

$$(x'_1 + X'_1) = (x'_2 + X'_2) \text{……………………………………..…. (27)}$$

$$(X'_1 - X'_2) = -(x'_1 + x'_2) \text{……………………………….…..… (28)}$$

Another deterministic criterion to measure the impact is the coefficient of restitution abbreviated as COR and it's a measure of the energy loss, which is the ratio of the speed differences after and before a collision

$$\text{COR} = \frac{(X'_1 - X'_2)}{(x'_1 + x'_2)} \text{…………………………...…….. (29)}$$

Where: always COR is less than one. When COR = 1, with no energy loss, the impact is said to be perfectly elastic. If COR = 0, the impact is said to be plastic, and the two colliding bodies remain in contact after impact with zero relative rebound velocity.

# Chapter 4

## 4.1. Modeling and Finite Element Analysis

### 4.1.1. Introduction

In the finite-element analysis (FEA), a computer model is developed to analyze a structure and this model is used in product design and improves the performance of existing products model. The finite-element analysis allows designers to know the design performance of the required specifications before the products are manufactured process. There are two kinds of finite-element analysis, these are:

- Two dimensional modeling analysis
- Three dimensional modeling analysis

The two dimensional modeling analysis is simple and permits computationally efficient analysis, it gives reduced accuracy, but three dimensional modeling gives more accurate result. The finite-element analysis considers the system as linear or nonlinear. Modeling a linear system is not as complex and usually does not consider plastic deformation, while nonlinear systems do take plastic deformation into account.

### 4.1.2. The Three Wheeled Bajaj Specification

The general specification of Bajaj RE Compact 4S is given in the table 4.1

Table 4.1. Specification of Bajaj RE Compact 4S [25]

| Specification | | |
|---|---|---|
| Seating Capacity | | 3 and driver |
| Max Power | | 8.1 kw@ 5000 rpm |
| Max Torque | | 18.0Nm @ 3500 rpm |
| Kerb weight | | 337 Kgs |
| Gearbox | | 4-Speed |
| Ground Clearance | | 200 mm |
| Over all Dimension | length | 2635 mm |
| | width | 1300 mm |
| | height | 1710 mm |
| Max. Speed | | 65 km/h |
| Chassis Type | | Monocoque |
| Suspension Type | | Double Acting Hydraulic Shock Absorber |

Figure 4. 1.Bajaj 4S overview [25]

### 4.1.3. Material for the Bumper

Glass fibers are the most common reinforcement for matrix composites. Their principal advantages are the relationship between their low cost, high tensile strength, high chemical resistance, and insulating properties. E-glass and S-glass are the types of fibers more commonly used in the fiber-reinforced plastic industry specifically in automotive industry. E-glass fibers have the lowest cost of all commercially available reinforcing GFs, which is the reason for their widespread use in the fiber-reinforced plastic industry. Material property of E-glass/Epoxy is determined through rule of mixture. Properties that obey this rule can be calculated as the sum of the value of the property of each constituent multiplied by its respective volume fraction or weight fraction in the mixture. In order to calculate properties by the rule-of-mixtures, the volume fraction or weight fraction of each constituent must first be determined.

- ✓ Volume fraction of the fiber component $V_f$ *is* defined as:

$$V_f = \frac{v_f}{v_c} \quad \ldots\ldots\ldots\ldots\ldots\ldots\ldots\ldots\ldots\ldots\ldots\ldots\ldots\ldots \text{(30)}$$

Where: $v_f$ is the volume of the fiber and $v_c$ is the volume of the composite.

- ✓ Volume fraction of the matrix component $V_m$ is defined as:

$$V_m = \frac{v_m}{v_c} \quad \ldots\ldots\ldots\ldots\ldots\ldots\ldots\ldots\ldots\ldots\ldots\ldots\ldots \text{(31)}$$

Where: $v_m$ is the volume of the matrix.

- ✓ In a two component system consisting of one fiber and one matrix, then, the total volume of the composite is

$$v_c = v_f + v_m \quad \ldots\ldots\ldots\ldots\ldots\ldots\ldots\ldots\ldots\ldots\ldots\ldots\ldots \text{(32)}$$

Similarly the weight fractions $W_f$ and $W_m$ of the fiber and matrix respectively can be defined in terms of the fiber weight ($w_f$), the matrix weight ($w_m$) and the composite weight ($w_c$).

$$W_f = \frac{w_f}{w_c} \quad \ldots\ldots\ldots\ldots\ldots\ldots\ldots\ldots\ldots\ldots\ldots\ldots\ldots \text{(33)}$$

$$W_m = \frac{w_m}{w_c} \quad \ldots\ldots\ldots\ldots\ldots\ldots\ldots\ldots\ldots\ldots\ldots\ldots\ldots \text{(34)}$$

$$W_f + W_m = 1 \ldots\ldots\ldots\ldots\ldots\ldots\ldots\ldots\ldots\ldots\ldots\ldots\ldots \text{(35)}$$

The composite density, or solution density, refers to the total density of a chemical mixture or composition of materials. If multiple substances are mixed into a homogeneous solution, the composite or solution density can be found by multiplying each substance's density by its solution concentration. [22]

The density of the composite in terms of volume fraction can be found by considering the weight of the composite to be composed of the weights of the constituent. The weights can be expressed in terms of their respective densities and volumes,

$$r_C v f = r_f v_f + r_m v_m \quad \text{.........................................} (36)$$

Applying the definitions of volume fraction the density of the composite, $rc$ can be expressed in terms of the fiber density, $r_f$ and the matrix density $r_m$ as

$$r_C = r_f V_f + r_m V_m \quad \text{.........................................} (37)$$

Hence the density of the composite can be very simply predicted using rule-of-mixtures based on volume fraction. The assumption will be the composites with zero voids. The composite density in terms of weight fraction can be found correspondingly by considering the volume of the composite to be composed of the volumes of their constituent, and by applying weight fractions gives

$$\rho_f = \frac{1}{\frac{W_f}{\rho_f} + \frac{W_m}{\rho m}} \quad \text{.........................................} (38)$$

The strength of a composite when measured in the direction of the fibers is referred to as the longitudinal strength. The stresses at which the fibers and the matrix fail determine the strength of a composite. The stresses in the unidirectional composite can be determined by taking an assumption. Thus are:

- ✓ The fibers are continuous
- ✓ The fibers are aligned in one direction only
- ✓ The load is applied parallel to the direction of the fibers

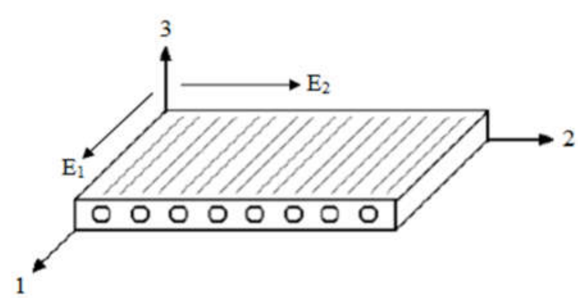


Figure 4. 2.Unidirectional composite lamina

✓ Determination of longitudinal tensile modulus for unidirectional ply (**$E_1$**)

The longitudinal tensile moduli of the composite material in the 1-direction, that is, in the fiber direction from the above figure and take different assumptions, thus are

- Fibers are uniform, parallel and continuous.
- Longitudinal load produces equal strain in fiber and matrix
- Perfect bonding between fiber and matrix.

The load applied in the fiber direction is distributed between fiber and matrix:

$$F_1 = F_f + F_m \quad \text{……………………………………………………………..(39)}$$

and stresses that act on the composite depend on the cross-sectional areas of fiber and matrix:

$$\sigma_1 A = \sigma_f A_f + \sigma_m A_m \quad \text{…………………………………………………. (40)}$$

Applying Hooke's law for the relationship of stress and strain:

$$E_1 \varepsilon_1 A = E_f \varepsilon_f A_f + E_m \varepsilon_m A_m \quad \text{………………………………………… (41)}$$

But the strain in fiber, matrix and composite are the same, so

$$E_1 A = E_f A_f + E_m A_m \quad \text{…………………………………………………. (42)}$$

$$E_1 = E_f\left(\frac{A_f}{A}\right) + E_m\left(\frac{A_m}{A}\right) \quad \text{………………………………………………(43)}$$

But from the above for the unidirectional ply, ($\frac{A_f}{A}$) and ($\frac{A_m}{A}$) are the same as volume fractions and the sum of the volume fractions of all constituents in a composite must equal to 1. The composite consisting of fiber and matrix, then, the total volume of the composite is

$$1 = v_f + v_m \quad \text{……………...…………………….(44)}$$

Substitute the equation in the above

$$E_1 = E_f v_f + E_m(1 - v_f) \quad \text{…………………………................................. (45)}$$

✓ Determination of transverse tensile modulus for unidirectional ply (**$E_2$**)

The transverse Young's modulus of the composite material in the 2 and 3-direction, that is in the transverse fiber direction $E_2$.and some assumptions are taken, thus are

- The same transverse stress $\sigma_2$ is applied to both the fiber and the matrix
- We cannot make an assumption on strains in fiber and in matrix in the 2 and 3-direction.
- Loads are applied at right angles to the fibers.
- Fibers are lumped together

The strains in the fiber and in the matrix are founded respectively:

$$\varepsilon_f = \frac{\sigma_2}{E_f} \quad \text{And} \quad \varepsilon_m = \frac{\sigma_2}{E_m} \quad \ldots\ldots (46)$$

$$\sigma_c = \sigma_f = \sigma_m = \sigma_2 \quad \ldots\ldots (47)$$

The strain or deformation of the entire composite is

$$\varepsilon_c = \varepsilon_f v_f + \varepsilon_m v_m \ldots\ldots (48)$$

But $\varepsilon = \sigma / E$

Therefore, directly substitute in to

$$\frac{\sigma_2}{E_2} = \frac{\sigma_2}{E_f} v_f + \frac{\sigma_2}{E_m} v_m \quad \ldots\ldots (49)$$

$$\frac{1}{E_2} = \frac{v_f}{E_f} + \frac{v_m}{E_m} \quad \ldots\ldots (50)$$

$$\frac{1}{E_2} = \frac{v_f}{E_f} + \frac{(1-v_f)}{E_m} \quad \ldots\ldots (51)$$

Therefore $E_2$

$$E_2 = \frac{E_f E_m}{E_m v_f + E_f(1-v_f)} \quad \ldots\ldots (52)$$

- ✓ Determination of Poisson's Ratio

The Poisson's ratio, $v_{12}$, is obtained by an approach similar to the analysis for $E_1$. The major Poisson's ratio is

$$v_{12} = -\frac{\varepsilon_2}{\varepsilon_1} \quad \ldots\ldots (53)$$

The fundamental simplifying assumption is that the fiber strains are identical to the matrix strains in the fiber direction, as in the approach to $E_1$. The transverse deformation $\Delta w$ is macroscopically

$$\Delta_W = \text{-w}\varepsilon_2 = \text{-w}v_{12}\varepsilon_1 \quad \text{.....................................................} (54)$$

But microscopically

$$\Delta_W = \Delta_{mW} + \Delta_{fW}$$

$$\Delta_{mW} = \text{w}V_m v_m \varepsilon_1 \quad \text{and} \quad \Delta_{fW} = \text{w}V_f v_f \varepsilon_1 \text{..........................................} (55)$$

Then we get

$$v_{12} = V_m v_m + V_f v_f \quad \text{And} \quad v_{21} = \frac{E_{22}}{E_{11}} v_{12} \text{..........................................} (56)$$

- ✓ Determination of shear modulus

The shear modulus of a lamina, $G_{12}$, is determined through considering the shearing stresses on the fiber and on the matrix are the same.

$$\gamma_m = \frac{\tau}{G_m} \quad \text{And} \quad \gamma_f = \frac{\tau}{G_f}$$

The total shear deformation on a macroscopic

$$\Delta_m = \text{w}V_m v_m \gamma_m \quad \text{and} \quad \Delta_f = \text{w}V_f v_f \gamma_f \quad \text{..........................................} (57)$$

Therefore from the above relation

$$\gamma = V_m \gamma_m + V_f \gamma_f$$

$$\frac{\tau}{G_{12}} = V_m \frac{\tau}{G_m} + V_f \frac{\tau}{G_f} \text{..........................................................................} (58)$$

$$G_{12} = \frac{G_m G_f}{G_f v_m + G_m v_f)} \text{..........................................................................} (59)$$

Therefore the strengths, stiffness's, and hydrothermal properties of a laminate will depend on

- ✓ Elastic modules
- ✓ Angle of orientation
- ✓ Stacking position
- ✓ Coefficients of thermal expansion
- ✓ Thickness

Therefore from the above theoretical background and appendix -1we get the material property of E-Glass Epoxy as follows in table 4. 1

Table 4. 2.Material property of E-glass/Epoxy appendix -1 and [14]

| Material type | Material property | | | |
|---|---|---|---|---|
| | Property | | unit | Values |
| E- glass/Epoxy composite | Tensile modulus(E) | x-direction ($E_x$) | MPa | 34000 |
| | | y-direction ($E_y$) | MPa | 65300 |
| | | z-direction ($E_z$) | MPa | 65300 |
| | Tensile strength($\sigma$) | longitudinal ($\sigma$) | MPa | 490 |
| | | transverse ($\sigma$) | MPa | 900 |
| | Compressive strength ($\sigma$) | longitudinal ($\sigma$) | MPa | 300 |
| | | transverse ($\sigma$) | MPa | 450 |
| | Shear modulus( $\tau$) | xy-direction ( $\tau_{xy}$) | MPa | 2433 |
| | | yz-direction ( $\tau_{yz}$) | MPa | 1698 |
| | | zx-direction ( $\tau_{zx}$) | MPa | 2433 |
| | Poisson ratio | xy-direction ( $\mu_{xy}$) | - | 0.217 |
| | | yz-direction ( $\mu_{yz}$) | - | 0.366 |
| | | zx-direction ( $\mu_{zx}$) | - | 0.217 |
| | Density ($\rho$) | - | $kg/mm^3$ | $2.6*10^6$ |
| | Flexural modulus ($E_{bend}$) | - | MPa | 40000 |
| | Flexural strength ($\sigma_{failur}$) | - | MPa | 1200 |

Arrangement of the glass fiber shows how the individual strands are positioned and this determines both direction and level of strength achieved in a molded. From the three basic arrangements of glass fiber reinforcement, the best directional arrangement is multi directional or random arrangements provide essentially equal strength in all directions of the finished part and gives resistance of the load at each point is equally distributed .But in case of the frontal and rear bumper the impact acted in axial direction, so a unidirectional fiber arrangements provide essentially equal strength in the longitudinal directions of the finished part and gives resistance of the load at the impact direction .

### 4.1.4. Modeling of the Three Wheeled Bajaj Bumper

For the purpose of the bumper structure, we use a honeycomb sandwich structure with hexagonal and rectangular geometry that consists of thin, stiff and strong faces separated by a relatively thick lightweight core. The basic criteria for selecting the structure are to achieve stiff and simultaneously light component. Important characteristics for honeycomb sandwich structures are:

- ✓ Lightweight compared to metallic
- ✓ High stiffness
- ✓ Cost effective

The general geometric parameters of the honeycomb cell is given in the table below in table 4. 3

Table 4. 4.Design Parameters of the honeycomb

| General geometric parameters of the honeycomb of unit cell(Hexagonal shape) | |
|---|---|
| Geometric parameters | Dimension |
| Height of cell | 20mm |
| Inclined length of cell | 20mm |
| Thickness of cell wall | 5mm |
| Cell angel (θ) | $30^0$ |
| Core shape | Hexagonal |

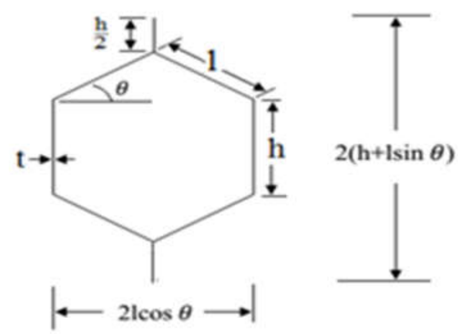


Figure 4. 3.Geometric of hexagonal unit cell

| General geometric parameters of the honeycomb of unit cell(Rectangular shape) | |
|---|---|
| Geometric parameters | Dimension |
| Height of cell | 20mm |
| Length of cell | 20mm |
| Thickness of cell wall | 5mm |
| Cell angel (θ) | $90^0$ |
| Core shape | Rectangular |

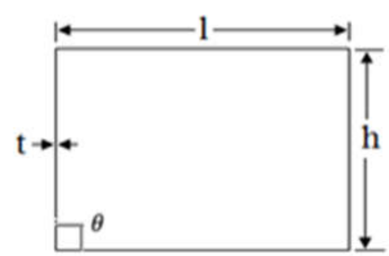


Figure 4. 4.Geometric of rectangular unit cell

The overall dimension of the bumper model given in the table 4.4

Table 4. 5.Dimension of the bumper model

| Parameters | | Front Bumper Model | Rear Bumper Model |
|---|---|---|---|
| Over all Dimension | Length | 1300 mm | 1300mm |
| | Width | 80mm | 70mm |
| | Height | 150mm | 150mm |

### 4.1.4.1. Create a model

Using ABAQUS/CAE 6.13 to create a three-dimensional model of the honeycomb bumper structure with hexagonal and rectangular geometry. The honeycomb bumper is constructed with 80mm mm thick in case of front and 70mm in case of rear, 1300mm length and 150 mm height. The general dimension of the bumper for front and rear could be 1300 *80*150 mm and 1300 *70*150 mm for analysis respectively. The Created Parts of the bumper are

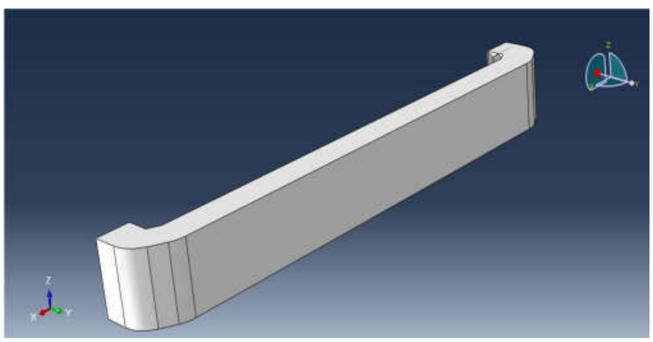

Figure 4. 5. (a) Hexagonal honeycomb bumper for front and rear impact (front view)

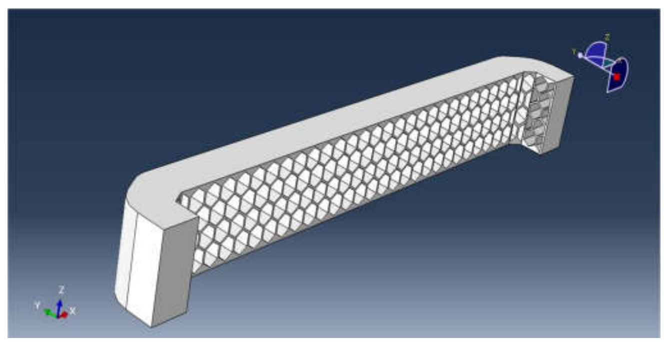

Figure 4.6. (b) Hexagonal honeycomb bumper for front and rear impact (rear view)

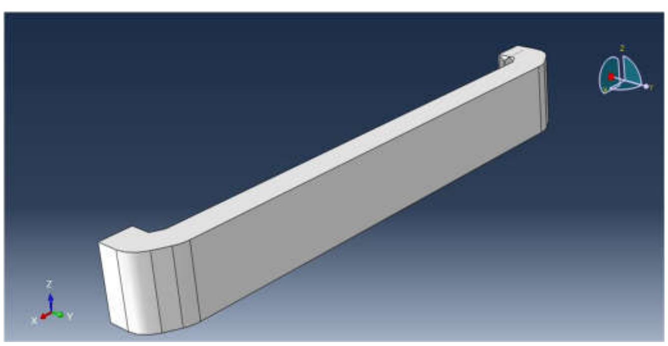

Figure 4.6. (a) Rectangular honeycomb bumper for front and rear impact(front view)

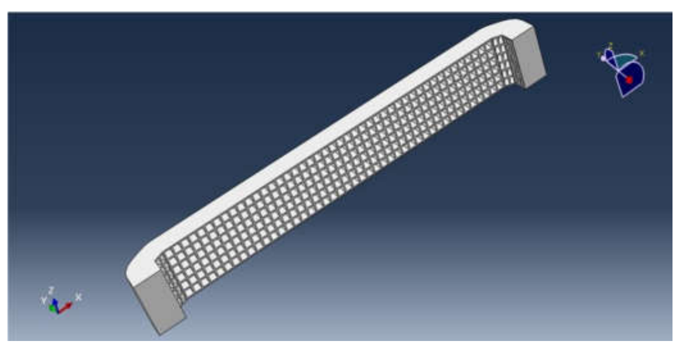

Figure 4.6. (b) Rectangular honeycomb bumper for front and rear impact (rear view)

#### 4.1.4.1. Finite element modeling

Finite element modeling is made with Ansys Workbench 16. The bumper model was made by using Abaqus CAE 6.13 software and imported to Ansys workbench 16.

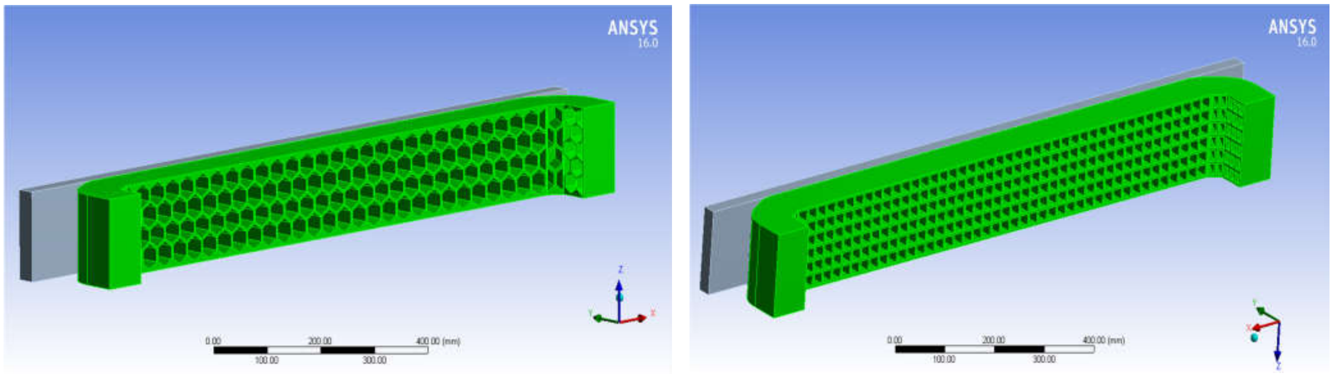


Figure 4. 7.Bumper imported model for hexagonal and rectangular geometry respectively

#### 4.1.4.2. Defining the material properties in Ansys workbench 16

Define the material and section properties. The model is made of E-Glass epoxy composite, with different material properties. The material is an orthotropic with a general property in different direction. The composite material and its layup were created by using Autodesk Helius Composite 2016.

Properties of Outline Row 4: E-Glass/Epoxy composite material

| | A | B | C | D | E |
|---|---|---|---|---|---|
| 1 | Property | Value | Unit | | |
| 2 | Density | 2.6E+06 | kg mm^-3 | | |
| 3 | Orthotropic Elasticity | | | | |
| 4 | Young's Modulus X direction | 21699 | MPa | | |
| 5 | Young's Modulus Y direction | 46185 | MPa | | |
| 6 | Young's Modulus Z direction | 21699 | MPa | | |
| 7 | Poisson's Ratio XY | 0.253 | | | |
| 8 | Poisson's Ratio YZ | 0.3728 | | | |
| 9 | Poisson's Ratio XZ | 0.253 | | | |
| 10 | Shear Modulus XY | 2433 | MPa | | |
| 11 | Shear Modulus YZ | 1698 | MPa | | |
| 12 | Shear Modulus XZ | 2433 | MPa | | |
| 13 | Field Variables | | | | |

Figure 4. 8.Material properties

### 4.1.4.3. Considering the frictional effect in finite element modeling of the bumper

Friction can be defined as resistance to relative motion of contacting bodies. Currently the value of the coefficient of friction was found as constant for each class of materials. The different operating parameters that change frictions are applied load or contact pressure, wear rate and surface roughness [22]. In general contact is the study of deformable bodies that touch each other at least one point in the space. Coefficient of friction, μ for dry contact is about 0.42 and for lubricated contact are ranges from 0.029-0.1 depending on the lubricant viscosity. For any three dimensional objects in contact on shared point or surface, the friction stresses that arise during shared point or surface contact between deformable bodies. Depending on geometry and material properties of each deformable body, contact can be an extremely non-linear event. In general, contacting pairs very often undergo non-linear plastic and permanent deformations, and thus Ansys comes with a selection contact computational algorithms to deal with contact definitions with a contact interaction property between the model and the rigid wall is defined using frictional coefficient behavior with friction coefficient of 0.3.

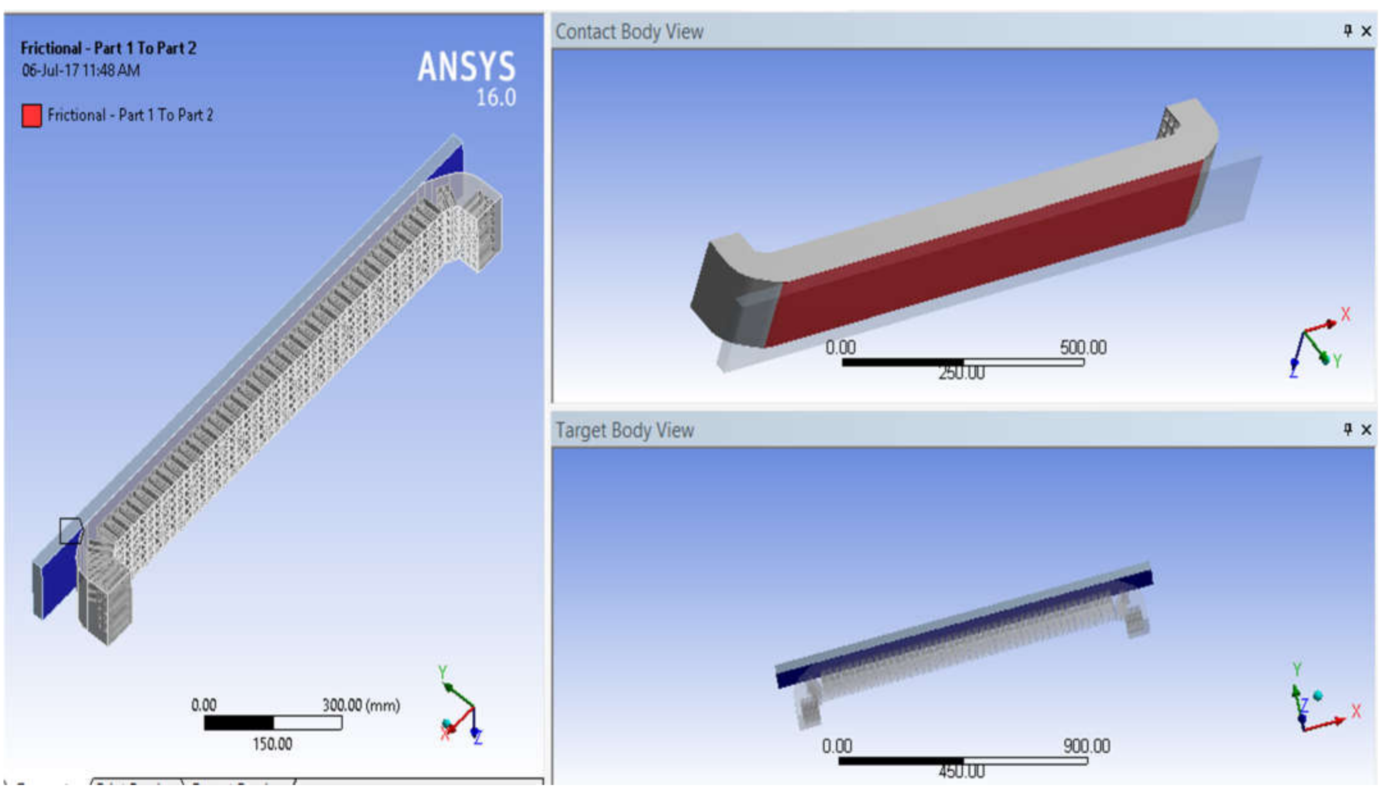


Figure 4. 9.Interaction property of the model

### 4.1.4. 4. Meshing the model

The Mesh module provides a variety of tools that allows to specify different mesh characteristics, such as mesh density, element shape and element type. The overall model is meshed with 43081 elements and 11437 nodes have been generated on the model.

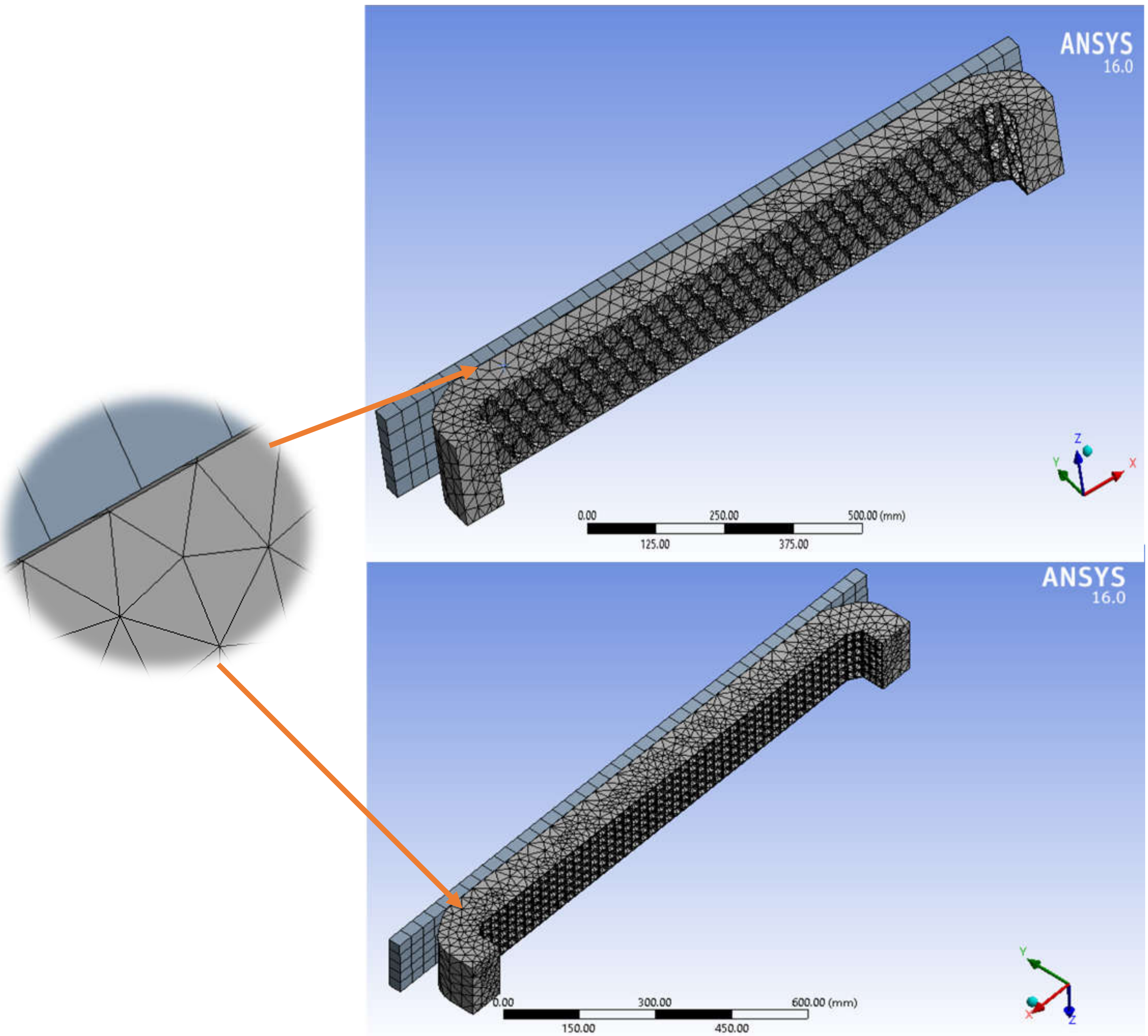


Figure 4. 10.Meshed model

### 4.1.4. 5. Inputs for Finite Element Analysis

The input for the finite element analysis is the velocity of the bumper. This input is applied during operation. There are different inputs in case of analysis steps that act on the bumper model and the fixed rigid wall. But the main input in this case is velocity of the bumper due to the movement of the bumper. When the analysis is carried out the displacement in vertical direction at the edge of the bumper is constrained.

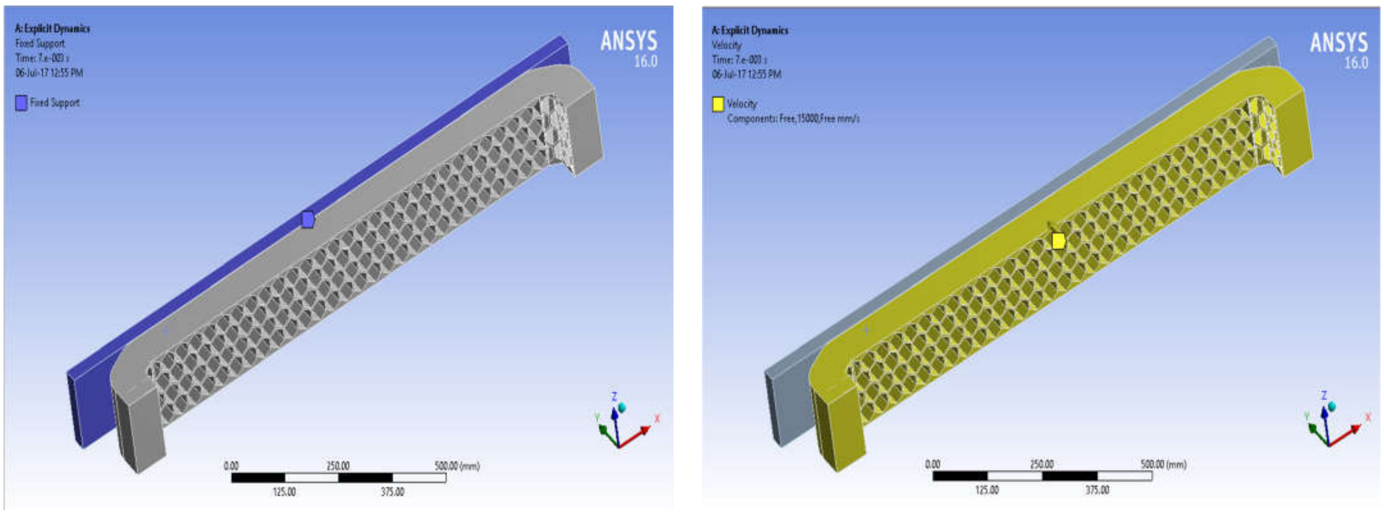


Figure 4. 11.Input parameters and boundary conditions

### 4.1.4.6. Applying the Boundary condition and initial velocity

Create boundary conditions that minimally constrain the movement of the bottom surface of the model and prevent rigid body motion ,so initial boundary conditions and the predefined velocity in the longitudinal direction (in y-direction) is applied at this step. The boundary condition are created using the displacement along the z-direction is constrained, the rigid wall movement is fixed so ($U_1$=$U_2$=$U_3$=$UR_1$=$UR_2$=$UR_3$=0) as boundary condition and in the predefined field with a varying velocity of 15m/s and 20 m/s in the y-axis that means

<u>Case 1</u>:-$V_1$=$V_3$= 0 and $V_2$= 20m/s

<u>Case 2</u>:-$V_1$=$V_3$= 0 and $V_2$= 25m/s

# Chapter 5

## 5.1. Results and discussion

In the previous chapter, steps and input parameters that are used in the analysis of the explicit dynamics are discussed briefly. In this chapter, a result of the analysis in relation to input parameters is discussed. The parameters that are specified in the previous chapter to give the result that change the bumper model analysis when it is exposed to these input parameters. In the analysis step, we are considering the effect of the velocity on the bumper model with different geometrical shapes.

The finite element model is generated in the ANSYS 16 software and the stresses, deflections, and the energy absorption are obtained. The results are taken for both the hexagonal geometry and rectangular geometry of the bumper model using E-Glass/Epoxy material. The effect of geometry and velocity are taken into consideration. The explicit dynamic analysis is mainly considered for analysis the bumper model. This will clearly explain the result of the bumper.

The analysis is carried out by three variations as follows.

- ✓ The variation of load applied in terms of velocity on the bumper.
- ✓ The variation of cell angle in geometry.
- ✓ The variation of geometry in the bumper model.
- ✓ Performing the model analysis.

### 5.1.1. Results

1. Result of equivalent (von-Misses) stress distributions and the total deformation on the bumper model with a velocity 20 m/s along with the direction of the impact with a fixed wall in hexagonal geometrical shapes

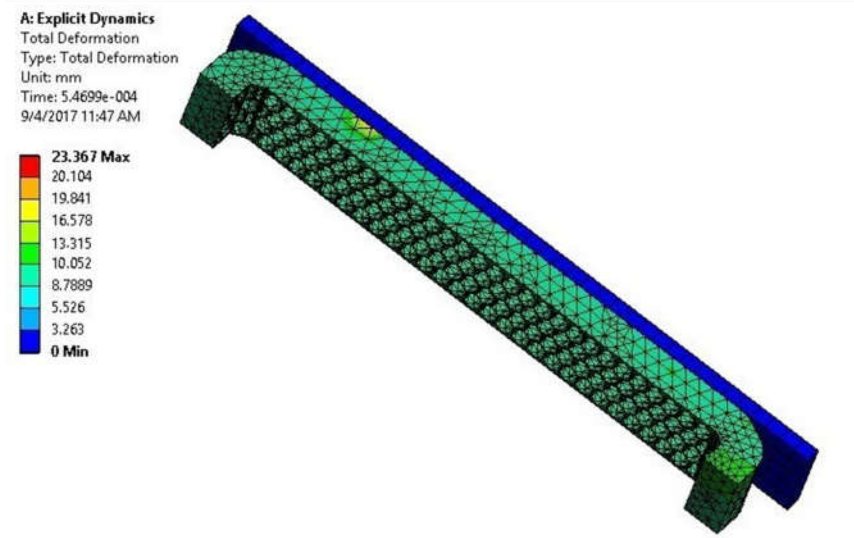


Max total deformation = 23.367 mm

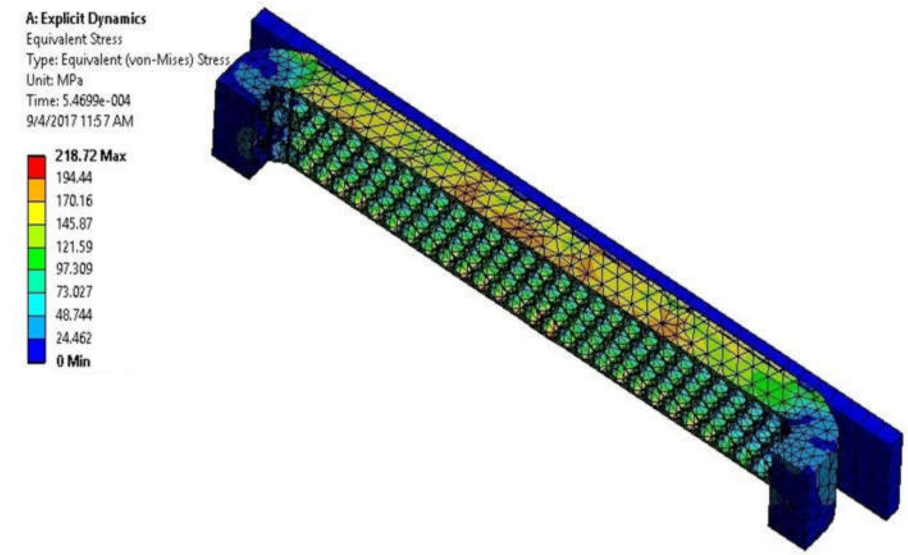


Max equivalent (von-misses) stress = 218.72 Mpa

Figure 5. 1.Analysis result of the hexagonal bump model with a velocity of 20m/s and 25m/s respectively

The total deformation and von-Misses stress value of the hexagonal geometry with an applied input velocity of 20m/s is shown in the above figures. So from the above figures we get the result of total deformation and von-Misses stress value, but the result is varies when the impact time rise. The total maximum deformation and von-Misses stress on the hexagonal geometry is 23.367 mm and 218.72 Mpa respectively.

2. Result of equivalent (von-Misses) stress distributions and the total deformation on the bumper model with a velocity 25 m/s along with the direction of the impact with a fixed wall in hexagonal geometrical shapes

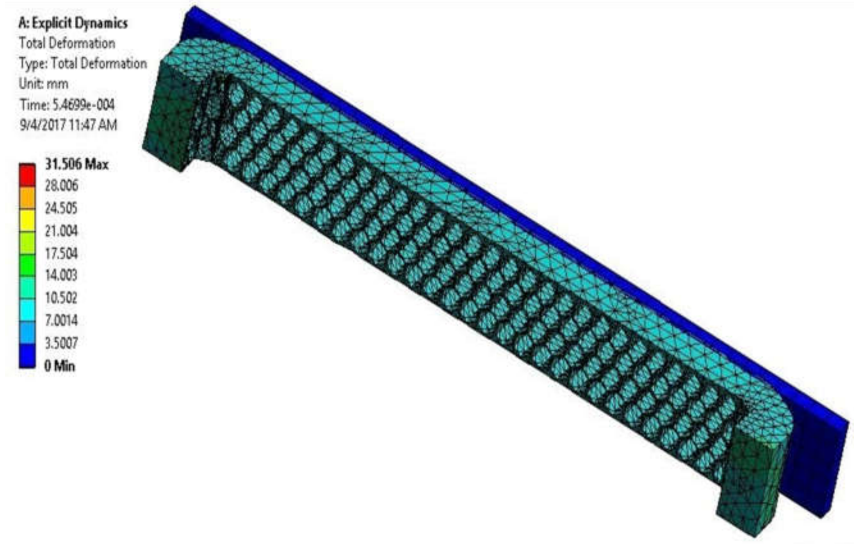


Max total deformation = 31.506 mm

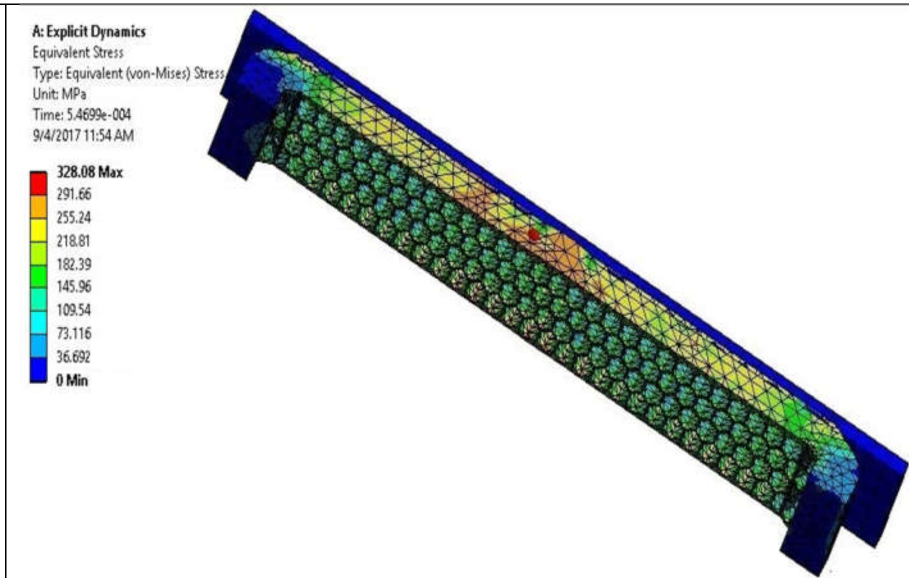


Max equivalent (von-misses) stress = 328.08 Mpa

Figure 5. 2.Analysis result of the rectangular bump model with a velocity of 20m/s and 25m/s respectively

The total deformation and von-Misses stress on the hexagonal geometry with an applied input velocity of 20m/s is shown in the above figures. So from the above figures we get the result of total deformation and von-Misses stress value, but the result is varies when the impact time rise. The total maximum deformation and von-Misses stress on the hexagonal geometry is 31.506 mm and 328.08 Mpa respectively.

3. Result of equivalent (von-Misses) stress distributions and the total deformation on the bumper model with a velocity of 20 m/s along with the direction of the impact with a fixed wall in rectangular geometrical shapes

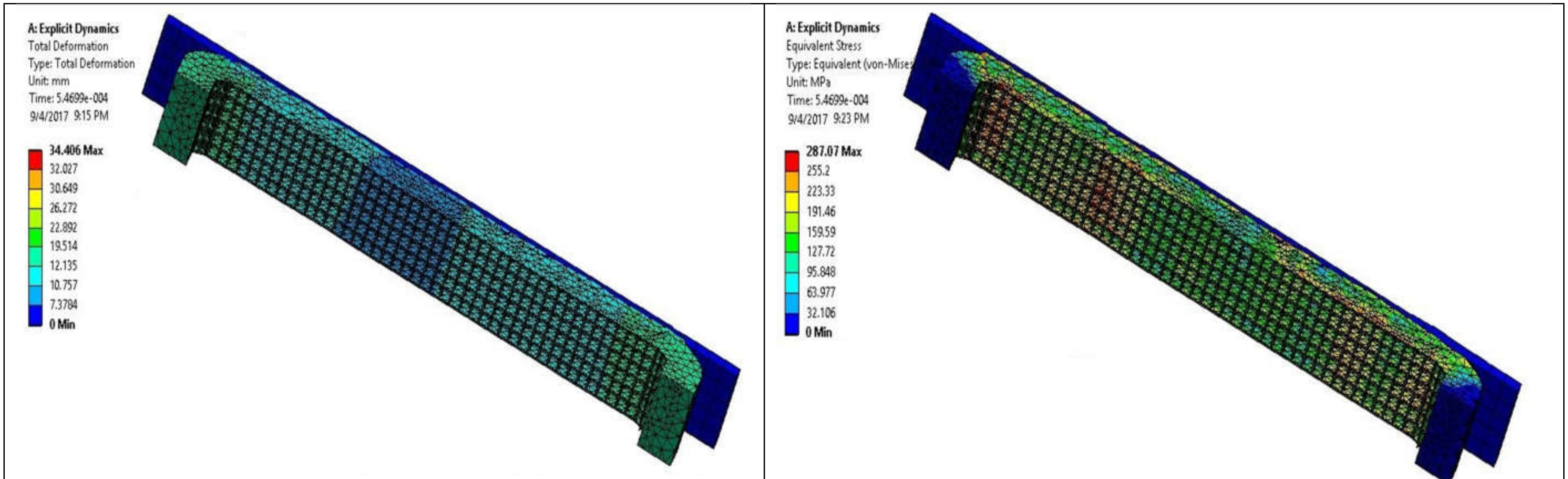


Max total deformation = 34.406 mm

Max equivalent (von-misses) stress = 287.07 Mpa

Figure 5. 3.Analysis result of the rectangular bump model with a velocity of 20m/s and 25m/s respectively

The total deformation and von-Misses stress on the rectangular geometry with an applied input velocity of 20m/s is shown in the above figures. So from the above figures we get the result of total deformation and von-Misses stress value, but the result is varies when the impact time rise. The total maximum deformation and von-Misses stress on the rectangular geometry is 34.406 mm and 287.07 Mpa respectively.

4. Result of equivalent (von-Mises) stress distributions and the total deformation on the bumper model with a velocity of 25 m/s along with the direction of the impact with a fixed wall in rectangular geometrical shapes

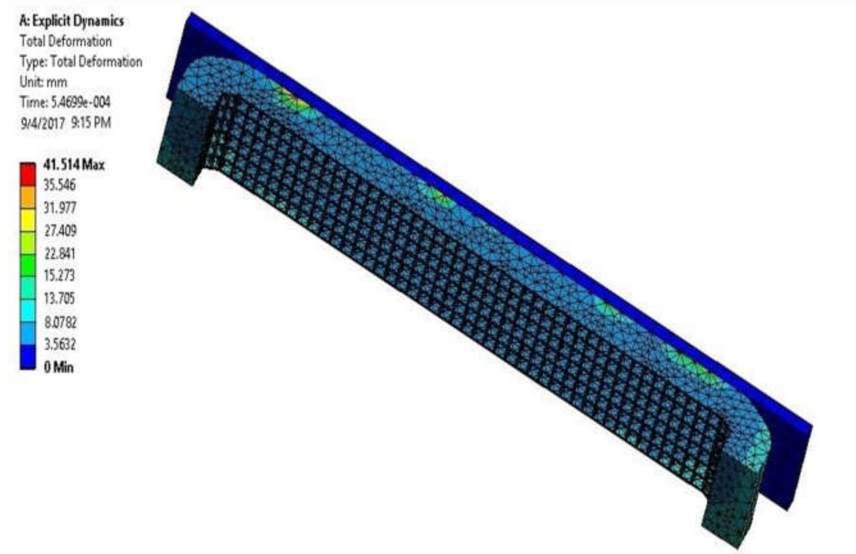


Max total deformation = 41.514 mm

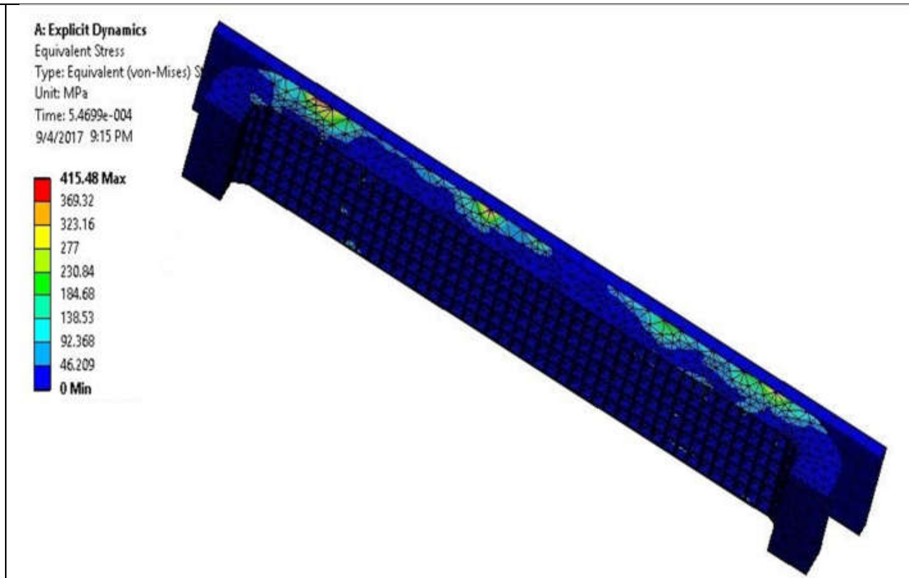


Max equivalent (von-misses) stress = 415.48 Mpa

Figure 5. 4.Analysis result of the rectangular bump model with a velocity of 20m/s and 25m/s respectively

The total deformation and von-Misses stress on the rectangular geometry with an applied input velocity of 20m/s is shown in the above figures. So from the above figures we get the result of total deformation and von-Misses stress value, but the result is varies when the impact time rise. The total maximum deformation and von-Misses stress on the rectangular geometry is 41.514 mm and 415.48 Mpa respectively.

5. Result of total internal energy absorption of the bumper model with a velocity of Velocity of 20 m/s along with the direction of the impact with a fixed wall in rectangular and hexagonal geometrical shapes

| Bumper model with a hexagonal geometry shape | Bumper model with a rectangular geometry shape |
|---|---|
| 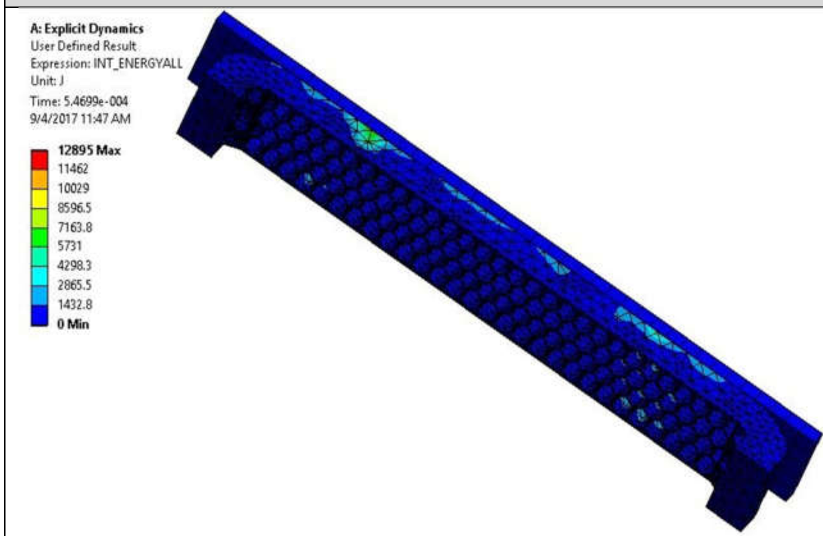 | 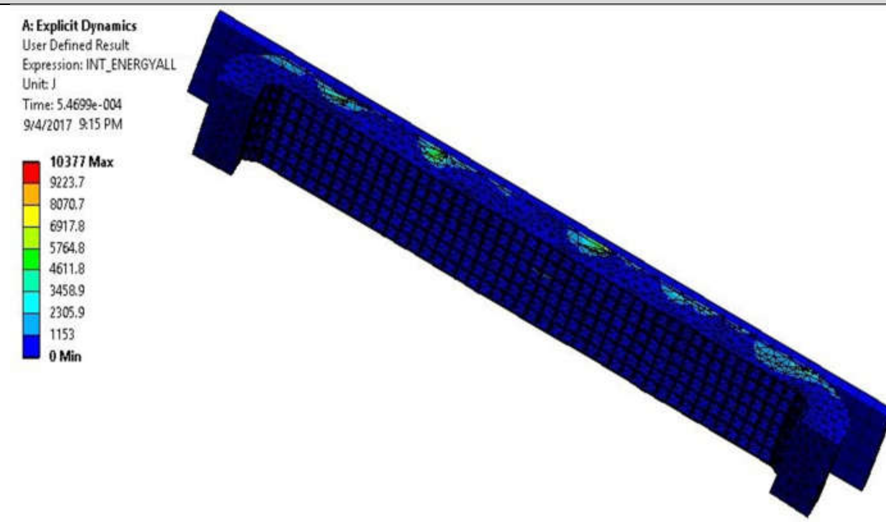 |
| Max internal energy = 1.2895e4J | Max internal energy = 1.0377e4J |

Figure 5. 5.Analysis result of the rectangular and hexagonal bump model with a velocity of 20m/s and 25m/s respectively

From the above figure, the bumper model with hexagonal geometry absorbed the more energy than that of rectangular geometry during the impact time. So from the above result the maximum energy absorbed by the hexagonal and rectangular bumper models are 1.2895e4J and 1.0377e4J respectively. Therefore, the maximum specific energy absorption of the hexagonal and rectangular bumper model are 939.88 J/Kg and 556.41 J/Kg, respectively. That means the above result shows that the hexagonal bumper model has high specific energy absorption than rectangular bumper models due to geometrical shape and the cell angle, therefore hexagonal bumper model higher specific energy absorption.

6. Result of total internal energy of the bumper model with a velocity of Velocity of 25 m/s along with the direction of the impact with a fixed wall in rectangular and hexagonal geometrical shapes

| Bumper model with a hexagonal geometry shape | Bumper model with a rectangular geometry shape |
|---|---|
| 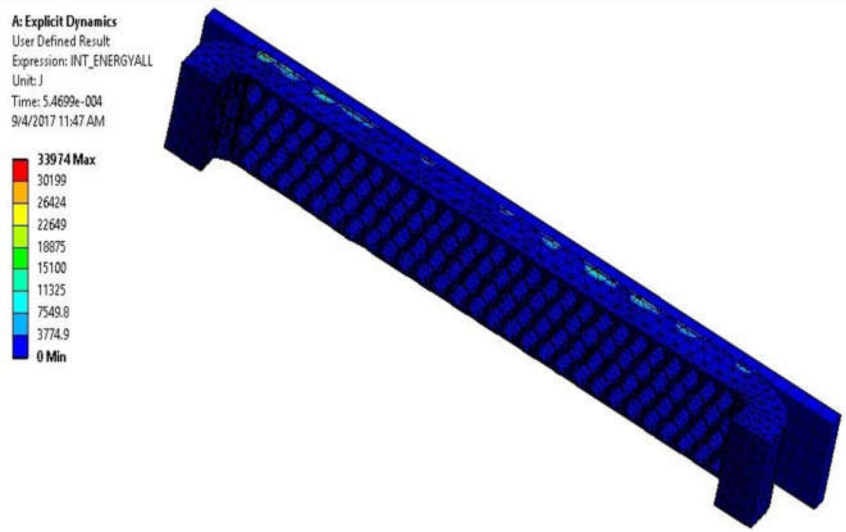 | 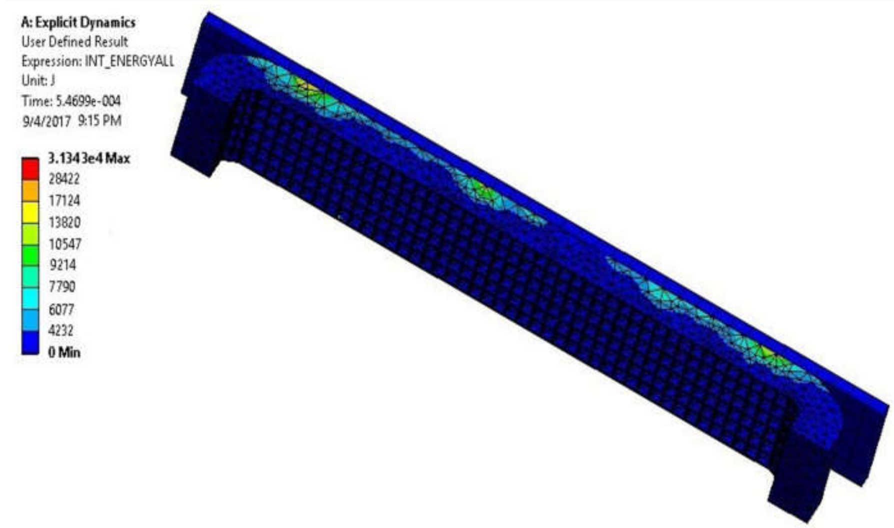 |
| Max internal energy = 3.3974e4J | Max internal energy = 3.1343e4J |

Figure 5. 6.Analysis result of the hexagonal and rectangular bump model with a velocity of 20m/s and 25m/s respectively

From the above figure, the bumper model with hexagonal geometry absorbed the more energy than that of rectangular geometry during the impact time. So from the above result the maximum energy absorbed by the hexagonal and rectangular bumper models are 1.2895e4J and 3.1343e4J respectively. Therefore the maximum specific energy absorption of the hexagonal and rectangular bumper model are 1137.53 J/Kg and 1075.45 J/Kg, respectively. That means the above result shows that the hexagonal bumper model has high specific energy absorption than rectangular bumper models due to geometrical shape and the cell angle, therefore hexagonal bumper model has higher specific energy absorption.

### 5.1.2. Discussion of the result

Using the ANSYS Workbench software, along with the boundary conditions, applied velocity is given along the impact direction with the fixed wall, and then we got a value for equivalent (von-Mises) stress, total deformation and total energy absorption. These three values are the result out puts.

1. The total deformation is the transformation of a bumper model from an initial or starting configuration to a current configuration with an application in terms of the velocity. That means the configuration is a set containing the positions of the bumper model at the moment of impact with the wall.

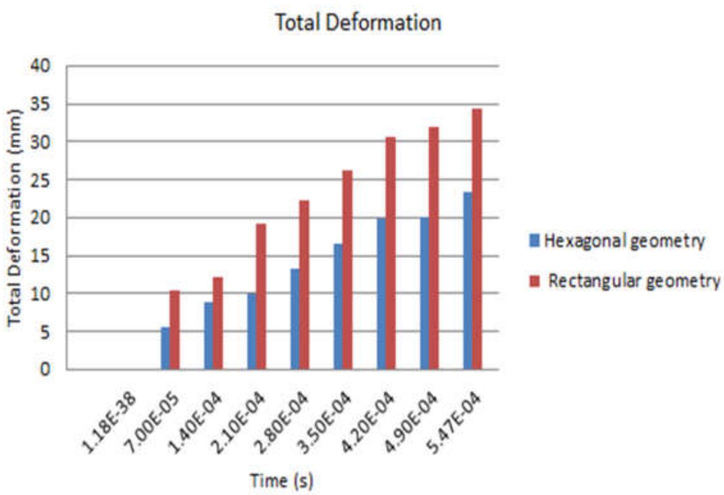


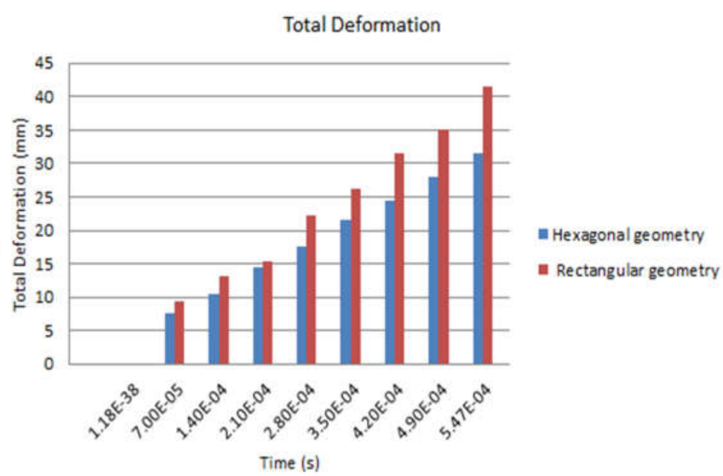


Figure 5. 7.Graphical representation of the total deformation analysis result for the hexagonal and rectangular bump model with a velocity of 20m/s and 25m/s respectively

The above figures show that the comparative geometrical deformation after the explicit dynamic analysis carried out. From the above graphical illustration the hexagonal bumper geometry has less deformation than the rectangular one with different time step. And also it shows that the deformation of the two bumper model increase when the duration of crash period increases, this means that the total deformation is directly related with the duration of the crash period. If the model has a larger crash period at the same time the total deformation of the model increases consequently.

2. The Von Misses stress is considered to be a safe for design analysis. The Von Misses stress information say the design will fail, if the maximum value of Von Misses stress induced in the material is more than strength of the material. So the von Misses stress is widely used to check whether their design will withstand given load

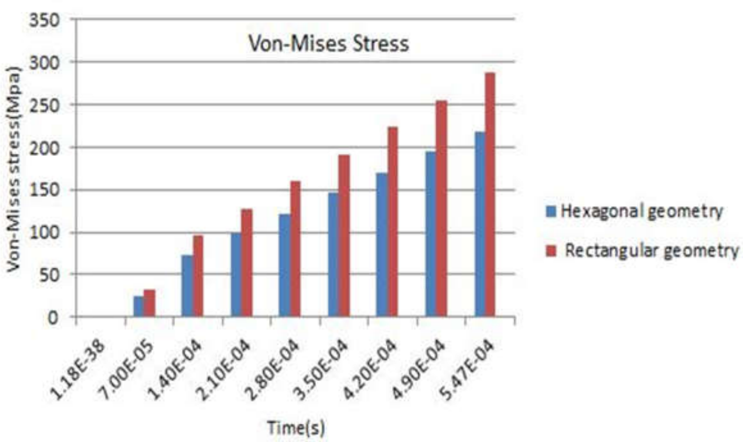


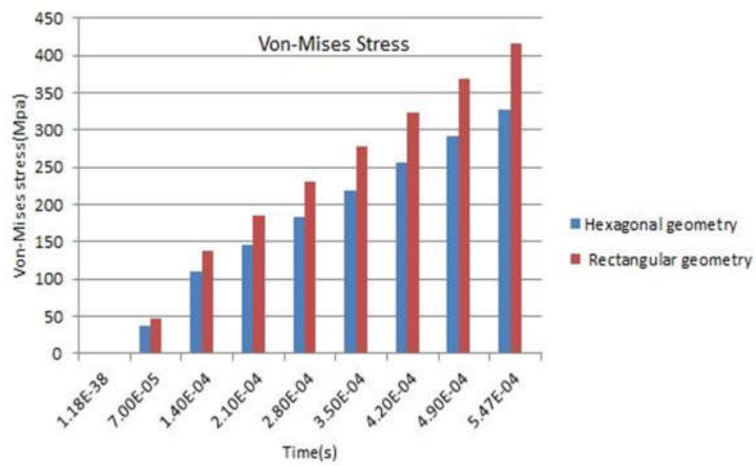


Figure 5. 8.Graphical representation of the von-mises stress analysis result for  the hexagonal and rectangular bump model with a velocity of 20m/s and 25m/s respectively

The above graphical representation taken out from the explicit dynamic analysis, it shows that the von-misses stress output results at different input conditions. According to the figure, when an increase in the time step the von misses stress increases due to the application of the load that take the duration due to an impact. When an increasing the time step the von misses stress value has been increases gradually in similar way when an increase in velocity the von misses stresses value produced in the bumper model also increase. So from the above result the von misses stress value distributions of hexagonal geometry bumper less than that the rectangular bumper, which means that hexagonal geometry bumper model is better than the rectangular bumper model.

3. The amount of energy that the bumper model absorbed during the entire impact analysis from start to end. The value is calculated from the time when the velocity begins to rise until the maximum time. This value can be used as an indicator to a materials toughness, that means the higher the value the stronger the material or the model.

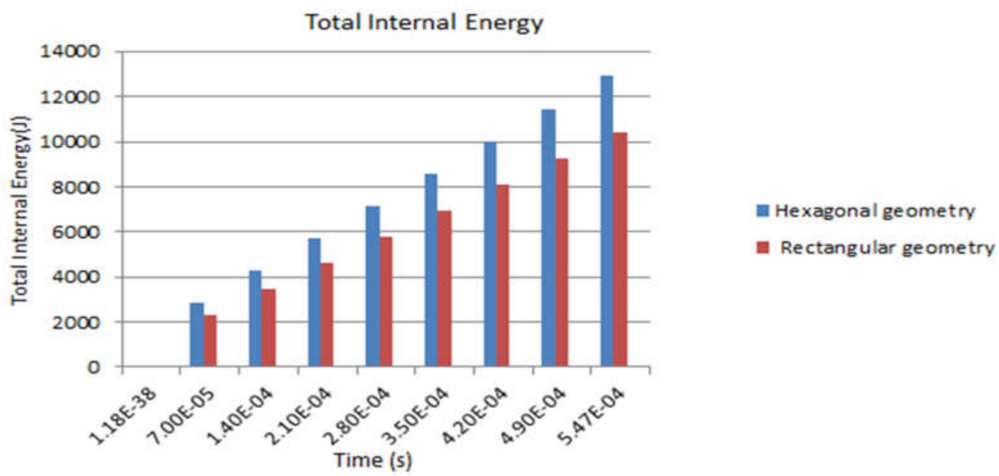


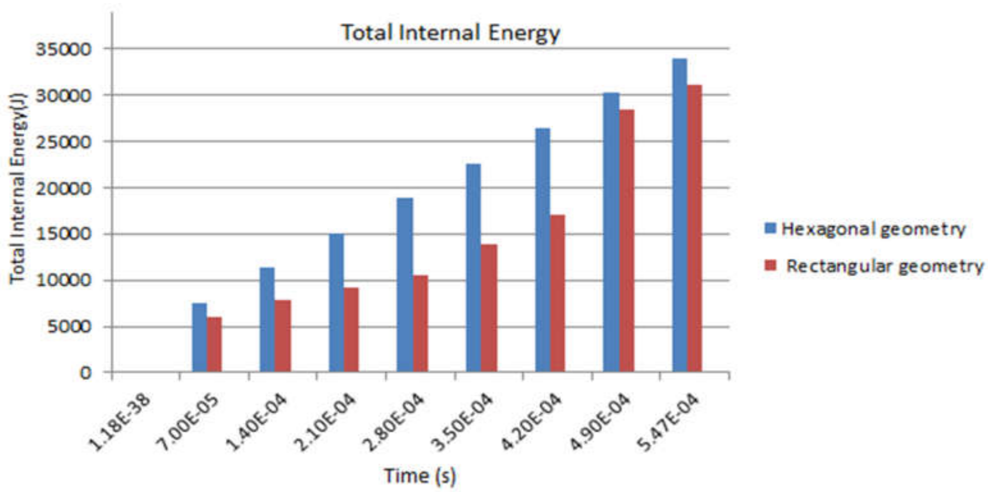


Figure 5. 9.Graphical representation of the total energy absorption analysis result for the hexagonal and rectangular bump model with a velocity of 20m/s and 25m/s respectively

The above graphical representation shows the internal energy absorbed by the hexagonal and rectangular bumper .Therefore the graphical representation shows that hexagonal bumper model is higher internal energy than the rectangular bump model during the impact period. And also the specific energy absorption of hexagonal bumper model is higher than the rectangular bump model during the impact period

Table 5. 1.Tabular representation of analysis result of hexagonal and rectangular bump model with a velocity of 20m/s and 25m/s respectively

| Explicit Dynamics Analysis | | |
|---|---|---|
| Criteria | Value | |
| Velocity = 20m/s | Hexagonal geometry | Rectangular geometry |
| Maximum deformation | 23.367mm | 34.406mm |
| Equivalent(von-Misses)stress | 218.72 Mpa | 287.07 Mpa |
| Total energy absorption | $1.2895*10^4$ J | $1.0377*10^4$ J |

| Explicit Dynamics Analysis | | |
|---|---|---|
| Criteria | Value | |
| Velocity = 25m/s | Hexagonal geometry | Rectangular geometry |
| Maximum deformation | 31.506mm | 41.514 mm |
| Equivalent(von-Misses)stress | 328.08 Mpa | 415.48 Mpa |
| Total energy absorption | $3.3974*10^4$ J | $3.1343*10^4$ J |

Table 5. 2. Comparison of hexagonal and rectangular bump model with a velocity of 20m/s and 25m/s

| Explicit Dynamics Analysis | | | | | | |
|---|---|---|---|---|---|---|
| Criteria | 20m/s | | | 25m/s | | |
| | Rectangular | Hexagonal | Percentage for Hexagonal | Rectangular | Hexagonal | Percentage for Hexagonal |
| Maximum deformation | 34.41mm | 23.37mm | - 46.1% | 41.514 mm | 31.506mm | - 31.77% |
| von-Misses stress | 287.07 Mpa | 218.72 Mpa | - 31.25% | 415.15 Mpa | 328.08 Mpa | - 26.54% |
| internal energy absorption | $1.0377*10^4$ J | $1.2895*10^4$ J | + 19.53% | $3.1343*10^4$ J | $3.3974*10^4$ J | +7.75% |
| specific energy absorption | 556.41 J/Kg | 939.88 J/Kg | + 40.88% | 1075.45 J/Kg | 1437.5 J/Kg | +25.19% |

The “+” and “-“sign are used for the percentage increase and decrease at the Explicit Dynamics Analysis criteria

# Chapter 6

## 6.1. Conclusions and Recommendation

### 6.1.1. Conclusions

This research focuses on the design and analysis of the bumper with different geometrical shapes for three wheeled vehicles. The energy absorption is the most important thing to be considered in the design process. The three wheeled vehicle bumper is modeled and analyzed by ANSYS Workbench FEM software. Since bumper model is subjected to an impact velocity of different magnitude and geometry, a rigid wall modeling is used for the analysis. The model is then analyzed by an explicit dynamic method using ANSYS Workbench 16.Among the two models (hexagonal and rectangular shapes) used for the explicit dynamic analysis, hexagonal geometrical bumper model possesses slightly lower Von Misses stress value and the lower deformation compared to rectangular geometry, which means that the hexagonal geometry is the better bumper model. During the impact analysis maximum internal energy absorption is obtained in the hexagonal geometry than the rectangular one, Hexagonal geometry also shows the lowest deformation and the highest internal energy absorption during the explicit dynamic analysis in comparison with rectangular geometry.

In the model analysis, the hexagonal geometry shows the higher specific energy absorption than the rectangular model. There for the result shows that hexagonal bumper model has high specific energy absorption, high internal energy absorption and least deformation as compared to rectangular bumper model. During explicit dynamic analysis, the hexagonal geometry gives the lower von misses stress value and deformation, due to the geometry of the model and the material that used in the analysis. Due to impact resistance of the material, E-glass epoxy composite is good where; the composites properties could be analyzed using Autodesk Helius Composite 2016 software. All the composite properties were exported from the Autodesk Helius Composite 2016 software to ANSYS Workbench 16. From the previous analysis, we can conclude that hexagonal geometry meets most of the requirements of high strength and higher stiffness than the rectangular one. The hexagonal geometry bumper model is used as the best and suitable models for minimization of injuries on the Bajaj component as well as humans during an accident than rectangular geometry.

### 6.1.2. Recommendation and Future Works

During the analysis of the bumper, there were a lot of problems to be solved. However, due to the broad applications of the bumper, the analysis is limited to the bumper analysis relating to the effect of impact velocity with a rigid body.

Based on the current and future accident in three wheeled vehicle and shortage of raw materials throughout the world, the broad study in minimizations of the injury and component failure invites the future works of different researchers. Among the potential area of problems that will be conducted, some of them are:

- ✓ Bumper chassis assembly optimization
- ✓ Design and analysis of different preventive mechanism
- ✓ Redesign of the three wheeled structure by considering best geometry
- ✓ Developing hybrid composite materials with high load impact resistance
- ✓ Minimization of the accident rate during rollover
- ✓ Impact testing of E-Glass Epoxy experimentally with different velocity
- ✓ Design and analysis of bumper using natural fibers
- ✓ Analyzing the effect of E-Glass Epoxy on environmental impact.

## Reference

[1]. Anoop Chawla, Sudipto Mukherjee and Dinesh Mohan, "Impact biomechanics in two wheeled and three wheeled vehicles," Indian Institute of Technology, New Delhi 110016 India, achawla@mech.iitd.ernet.in

[2]. Faizan Khatri, Sanchit Jain and Prof. P. Bhaskar, "Crash test simulation and analysis of a passenger bus frame" International Journal of Engineering Trends and Technology (IJETT), Vol-11, Number -1 -, May 2014, ISSN: 2231-5381

[3]. A Chawla, S Mukherjee, D Mohan, Rajiv Kumar and Tushar Gavade " FE simulation studies of a three-wheeled scooter taxi "Department of Mechanical Engineering, Indian Institute of Technology, New Delhi 110016 INDIA

[4]. Damtie Enawgew, "Strength analysis of three wheeled vehicle's chassis and body frame assembled in Ethiopia ", Addis Ababa Institute of Technology, Presented in partial fulfillment of the requirement for the Degree of Master of Science ,October, 2013

[5]. Ricardo, Miranda and S. Defljacov, "Procedures to apply finite elements analysis in automotive structures", J UNIFEI, São Bemardo Campo, University of São Paulo, CEP 09850-901, email: luiz.ricardo@poli.usp.br; renatcos@fei.edu br; sergiode@feLedu.br

[6]. Schmuesser D, Wickliffe L., "Impact energy absorption of continuous fiber composite tubes", J. Engng. Mat. & Tech, Vol. 109 (January 1987) p. 72-77.

[7]. Farley G. L., "Effect of fiber and matrix maximum strain on the energy absorption of composite materials", J. Comp. Mater., Vol. 20 (July 1986) p. 322-334.

[8]. George, John F, Srdan S and J. Michael "Energy absorption in polymer composite materials for automotive crashworthiness" Comp. Mater., p. 1-76.

[9]. S. Roth, D. Chamoret, J. Badin, JR. Imbert and S. Gomes "Crash FE simulation in the design process - theory and application" world's largest science, technology & medicine open access book publisher,Laboratoire M3M:, Université de Technologie de Belfort-Montbéliard, Cedex, 2DPS - Digital Product Simulation, France ,web:www.intechopen.com

[9]. S. Prabhakaran, K. Chinnarasu, M. Senthil Kumar"Design and Fabrication of Composite Bumper for Light Passenger Vehicles" International Journal of Modern Engineering Research (IJMER), Vol.2, 4, July-Aug 2012, pp-2552-2556

[10]. Pandey Alok S, Patil Nirav A and Nikumbh Pankaj S "Energy Absorbing Bumpers and it's Comparative Study" International Journal of Innovative Research in Science and Engineering (IJIRSE), Vol.2, 4, March 2016, pp-346 – 350

[11]. M. Anil Kumar and N. Phani Raja Rao "Design and Analysis of Car Bumper by Varying Materials and Speeds" International Journal on Recent Technologies in Mechanical and Electrical Engineering (IJRMEE), Vol.2, 4, March 2015, pp-056 – 061

[12] J. N. Reddy, An introduction to nonlinear finite element analysis, Oxford University Press, 2004

[13] Mariana Etcheverry and Silvia E. Barbosa, "Glass Fiber Reinforced Polypropylene Mechanical Properties Enhancement by Adhesion Improvement ", ISSN 1996-1944, www.mdpi.com/journal/materials, Vol.5, 4, 2012, pp- 1084-1113; doi: 10.3390/ma5061084

[14]. SushilB.C, Prof.K.M.Narkar, Pratik K "Design and Analysis of E-Glass/Epoxy Composite Mono leaf Spring for Light Vehicle" International Journal of Innovative Research in Science, Engineering and Technology (IJIRSET), Vol.4, 4, January 2015, pp- 18801 – 18808

[15]. P.K. Mallick "Fiber Reinforced Composites Materials, Manufacturing and Design, Marcel Dekker Inc, USA (1993).

[16]. M. Aktas "Temperature effect on impact behavior of laminated composite plates" Dissertation thesis, Dokuz Eylul University, 2007

[17]. netcompositesenterprise.com

[18]. K.L. Loewenstein, "The Manufacturing Technology of Continuous Glass Fibers", 3rd revised ed., Elsevier, 1993

[19]. D.M. Miller, "Glass Fibers Composites", Vol-1, Engineered Materials Handbook, ASM International, 1987, pp- 45- 48

[20]. "Standard Specification for Glass Fiber Strands", D 578-98, Annual Book of ASTM Standards, ASTM

[21]. Autar K. Kaw ,"Mechanics of Composite Materials" second edition ,2006 , CRC Press Taylor & Francis Group ,6000 Broken Sound Parkway NW, Suite 300 Boca Raton, FL 33487-2742

[22]. K. C. Ludema, "Hand book of lubrication theory and practice of tribology", CRC press, 1983

[23]. Muhammad S., Hambali A., Rosidah , Widodo W.S and Ahmad M.N," A Review of Energy Absorption of Automotive Bumper Beam", International Journal of Applied Engineering Research, Volume 12, Number 2, 2017, ISSN 0973-4562, pp. 238- 245

[24]. Getu S. Tulu , Simon Washington , Mark J. King ," Characteristics of Police-reported Road Traffic Crashes in Ethiopia over a Six Year Period", 2013 Australasian Road Safety Research, Policing & Education Conference 28th – 30th August, Brisbane, Queensland, pp. 1- 13

[25]. http://www.globalbajaj.com /re-4s/specifications. Accessed March 24, 2017.

## Appendix A

1. Determining the Lamina Properties of E-Glass Epoxy Composite

In designing composite materials, it is necessary to determine the properties of the composite for the fiber and matrix constituents. In this research we use the micromechanics tool in Helius Composite derive the properties of the lamina material property for a known fiber and matrix.

The micromechanics tool in Helius Composite uses a finite element model of fiber/matrix .The model uses the properties of the fiber and matrix along with the fiber volume fraction to calculate the properties of the composite.

1.1. Calculating Lamina Properties using Helius Composite

Calculating the lamina properties for a ply that containing E-Glass fiber and 5505 Epoxy matrix for different fiber volume and matrix volume ratio.

1. Determine the volume occupied by the fiber constituent.

2. Select the E-Glass in the fiber type.

3. Select the 5505 Epoxy in the matrix type.

4. Then enter the known matrix or fiber weight and the window should look like below.

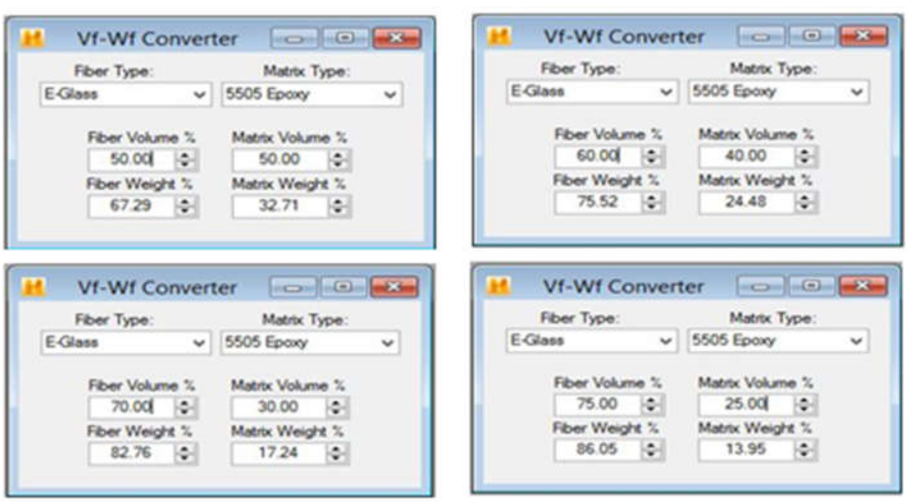


Figure 1: fiber and matrix ratio of E-Glass Epoxy

So we can now calculating the lamina properties.

1. Select the E-Glass in the fiber and 5505 Epoxy matrix materials on the Calculate tab.

2. Entering the previous fiber volume fraction from above and calculate.

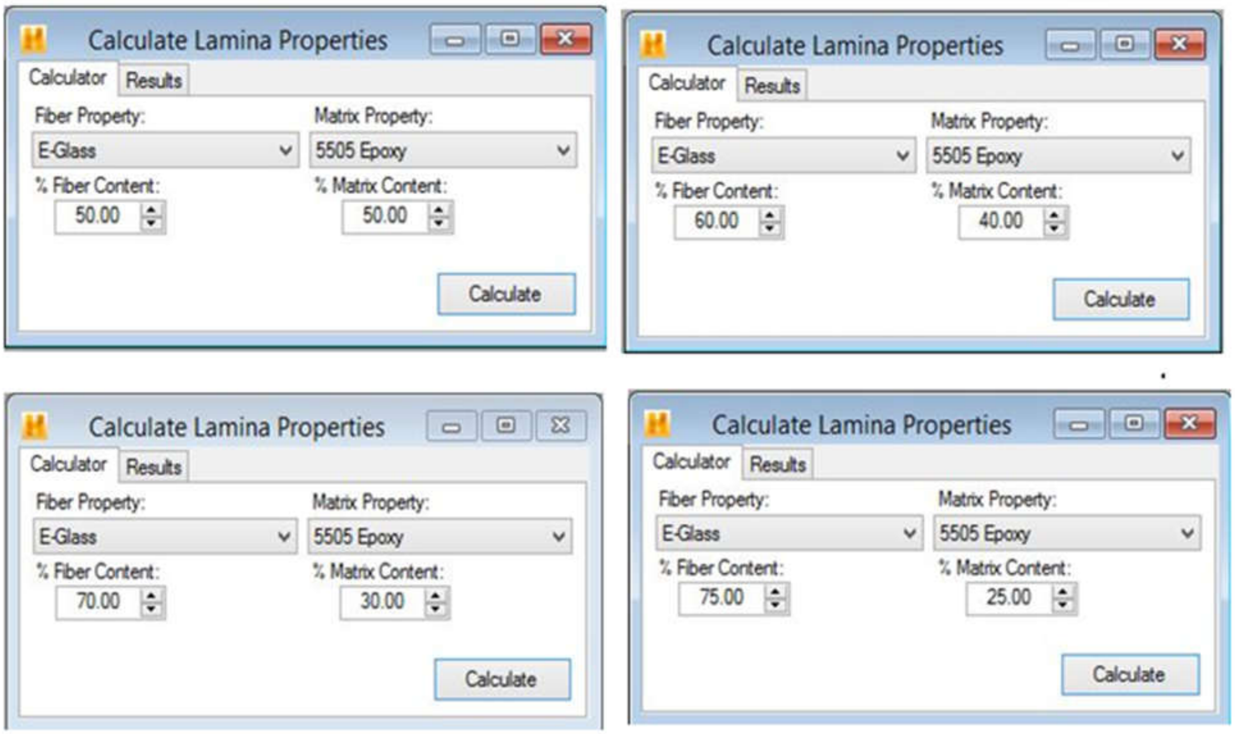


Figure 2: different ratio of fiber and matrix for calculating E-Glass Epoxy lamina properties

3. The results of the lamina properties should appear as shown below

Name: E-Glass Epoxy - 1

| Title | Value |
|---|---|
| Composite Type | Unidirectional |
| Fiber Vf | 5.00000E-01 |
| Thickness (mm) | 3.00000E-01 |
| E11 (MPa) | 3.97050E+04 |
| E22 (MPa) | 1.75452E+04 |
| E33 (MPa) | 1.75452E+04 |
| G12 (MPa) | 6.54023E+03 |
| G13 (MPa) | 6.54023E+03 |
| G23 (MPa) | 6.27091E+03 |
| NU12 | 2.67308E-01 |
| NU13 | 2.67308E-01 |
| NU23 | 4.00252E-01 |
| CTE1 (mm/mm/C) | 4.39251E-06 |
| CTE2 (mm/mm/C) | 2.06737E-06 |
| CTE3 (mm/mm/C) | 2.06737E-06 |
| CME1 (mm/mm/%m) | 0.00000E+00 |
| CME2 (mm/mm/%m) | 0.00000E+00 |
| CME3 (mm/mm/%m) | 0.00000E+00 |
| +S1 (MPa) | 1.07500E+03 |
| +S2 (MPa) | 5.76846E+01 |
| -S1 (MPa) | -7.25001E+02 |
| -S2 (MPa) | -1.72484E+02 |
| S12 (MPa) | 6.74918E+01 |
| +e1 (mm/mm) | 2.70747E-02 |
| +e2 (mm/mm) | 3.28777E-03 |
| -e1 (mm/mm) | -1.82597E-02 |
| -e2 (mm/mm) | -9.83086E-03 |
| e12 (mm/mm) | 1.03195E-02 |
| K1 (W/mm/K) | 6.41755E-04 |
| K2 (W/mm/K) | 0.00000E+00 |
| K3 (W/mm/K) | 0.00000E+00 |
| Density (g/mm3) | 1.93344E-03 |

Grayed out boxes are not required for basic mechanical analyses

Name: E-Glass Epoxy - 2

| Title | Value |
|---|---|
| Composite Type | Unidirectional |
| Fiber Vf | 6.00000E-01 |
| Thickness (mm) | 3.00000E-01 |
| E11 (MPa) | 4.61848E+04 |
| E22 (MPa) | 2.16986E+04 |
| E33 (MPa) | 2.16986E+04 |
| G12 (MPa) | 8.09538E+03 |
| G13 (MPa) | 8.09538E+03 |
| G23 (MPa) | 7.91302E+03 |
| NU12 | 2.52797E-01 |
| NU13 | 2.52797E-01 |
| NU23 | 3.72876E-01 |
| CTE1 (mm/mm/C) | 4.54270E-06 |
| CTE2 (mm/mm/C) | 2.66199E-06 |
| CTE3 (mm/mm/C) | 2.66199E-06 |
| CME1 (mm/mm/%m) | 0.00000E+00 |
| CME2 (mm/mm/%m) | 0.00000E+00 |
| CME3 (mm/mm/%m) | 0.00000E+00 |
| +S1 (MPa) | 1.29000E+03 |
| +S2 (MPa) | 5.97591E+01 |
| -S1 (MPa) | -8.70001E+02 |
| -S2 (MPa) | -1.78687E+02 |
| S12 (MPa) | 6.99576E+01 |
| +e1 (mm/mm) | 2.79313E-02 |
| +e2 (mm/mm) | 2.75406E-03 |
| -e1 (mm/mm) | -1.88374E-02 |
| -e2 (mm/mm) | -8.23498E-03 |
| e12 (mm/mm) | 8.64166E-03 |
| K1 (W/mm/K) | 7.70106E-04 |
| K2 (W/mm/K) | 0.00000E+00 |
| K3 (W/mm/K) | 0.00000E+00 |
| Density (g/mm3) | 2.06713E-03 |

Grayed out boxes are not required for basic mechanical analyses

Name: E-Glass Epoxy - 3

| Title | Value |
|---|---|
| Composite Type | Unidirectional |
| Fiber Vf | 7.00000E-01 |
| Thickness (mm) | 3.00000E-01 |
| E11 (MPa) | 5.26618E+04 |
| E22 (MPa) | 2.75627E+04 |
| E33 (MPa) | 2.75627E+04 |
| G12 (MPa) | 1.03296E+04 |
| G13 (MPa) | 1.03296E+04 |
| G23 (MPa) | 1.03106E+04 |
| NU12 | 2.38709E-01 |
| NU13 | 2.38709E-01 |
| NU23 | 3.39084E-01 |
| CTE1 (mm/mm/C) | 4.65824E-06 |
| CTE2 (mm/mm/C) | 3.25065E-06 |
| CTE3 (mm/mm/C) | 3.25065E-06 |
| CME1 (mm/mm/%m) | 0.00000E+00 |
| CME2 (mm/mm/%m) | 0.00000E+00 |
| CME3 (mm/mm/%m) | 0.00000E+00 |
| +S1 (MPa) | 1.50500E+03 |
| +S2 (MPa) | 6.21798E+01 |
| -S1 (MPa) | -1.01500E+03 |
| -S2 (MPa) | -1.85925E+02 |
| S12 (MPa) | 7.28349E+01 |
| +e1 (mm/mm) | 2.85786E-02 |
| +e2 (mm/mm) | 2.25594E-03 |
| -e1 (mm/mm) | -1.92740E-02 |
| -e2 (mm/mm) | -6.74555E-03 |
| e12 (mm/mm) | 7.05111E-03 |
| K1 (W/mm/K) | 8.98457E-04 |
| K2 (W/mm/K) | 0.00000E+00 |
| K3 (W/mm/K) | 0.00000E+00 |
| Density (g/mm3) | 2.20083E-03 |

Grayed out boxes are not required for basic mechanical analyses

Name: E-Glass Epoxy - 4

| Title | Value |
|---|---|
| Composite Type | Unidirectional |
| Fiber Vf | 7.50000E-01 |
| Thickness (mm) | 3.00000E-01 |
| E11 (MPa) | 5.58998E+04 |
| E22 (MPa) | 3.14357E+04 |
| E33 (MPa) | 3.14357E+04 |
| G12 (MPa) | 1.18791E+04 |
| G13 (MPa) | 1.18791E+04 |
| G23 (MPa) | 1.19246E+04 |
| NU12 | 2.31742E-01 |
| NU13 | 2.31742E-01 |
| NU23 | 3.20992E-01 |
| CTE1 (mm/mm/C) | 4.70636E-06 |
| CTE2 (mm/mm/C) | 3.54503E-06 |
| CTE3 (mm/mm/C) | 3.54503E-06 |
| CME1 (mm/mm/%m) | 0.00000E+00 |
| CME2 (mm/mm/%m) | 0.00000E+00 |
| CME3 (mm/mm/%m) | 0.00000E+00 |
| +S1 (MPa) | 1.61250E+03 |
| +S2 (MPa) | 6.34965E+01 |
| -S1 (MPa) | -1.08750E+03 |
| -S2 (MPa) | -1.89863E+02 |
| S12 (MPa) | 7.43999E+01 |
| +e1 (mm/mm) | 2.88463E-02 |
| +e2 (mm/mm) | 2.01989E-03 |
| -e1 (mm/mm) | -1.94545E-02 |
| -e2 (mm/mm) | -6.03972E-03 |
| e12 (mm/mm) | 6.26307E-03 |
| K1 (W/mm/K) | 9.62632E-04 |
| K2 (W/mm/K) | 0.00000E+00 |
| K3 (W/mm/K) | 0.00000E+00 |
| Density (g/mm3) | 2.26768E-03 |

Grayed out boxes are not required for basic mechanical analyses

Figure 3: different fiber and matrix ratio of E-Glass Epoxy lamina properties

4. Calculating the general lamina property of E-Glass Epoxy – 2 for the model by considering a single ply thickness

Table 3: sequencing each ply property of the model by considering a single ply thickness and orientation of the fiber

| Laminate : E-Glass Epoxy | | | |
|---|---|---|---|
| Ply# | Lamina | Thickness (mm) | Angle (deg.) |
| 1 | E-Glass Epoxy – 2 | 4.55 | $0^0$ |
| 2 | E-Glass Epoxy – 2 | 4.55 | $0^0$ |
| 3 | E-Glass Epoxy – 2 | 4.55 | $0^0$ |
| 4 | E-Glass Epoxy – 2 | 4.55 | $0^0$ |
| 5 | E-Glass Epoxy – 2 | 4.55 | $0^0$ |
| 6 | E-Glass Epoxy – 2 | 4.55 | $0^0$ |
| 7 | E-Glass Epoxy – 2 | 4.55 | $0^0$ |
| 8 | E-Glass Epoxy – 2 | 4.55 | $0^0$ |
| 9 | E-Glass Epoxy – 2 | 4.55 | $0^0$ |
| 10 | E-Glass Epoxy – 2 | 4.55 | $0^0$ |
| 11 | E-Glass Epoxy – 2 | 4.55 | $0^0$ |
| 12 | E-Glass Epoxy – 2 | 4.55 | $0^0$ |
| 13 | E-Glass Epoxy – 2 | 4.55 | $0^0$ |
| 14 | E-Glass Epoxy – 2 | 4.55 | $0^0$ |
| 15 | E-Glass Epoxy – 2 | 4.55 | $0^0$ |
| 16 | E-Glass Epoxy – 2 | 4.55 | $0^0$ |
| 17 | E-Glass Epoxy – 2 | 4.55 | $0^0$ |
| 18 | E-Glass Epoxy – 2 | 4.55 | $0^0$ |
| 19 | E-Glass Epoxy – 2 | 4.55 | $0^0$ |
| 21 | E-Glass Epoxy – 2 | 4.55 | $0^0$ |
| 22 | E-Glass Epoxy – 2 | 4.55 | $0^0$ |
| 23 | E-Glass Epoxy – 2 | 4.55 | $0^0$ |
| 24 | E-Glass Epoxy – 2 | 4.55 | $0^0$ |
| 25 | E-Glass Epoxy – 2 | 4.55 | $0^0$ |

| | | | |
|---|---|---|---|
| 26 | E-Glass Epoxy – 2 | 4.55 | $0^0$ |
| 27 | E-Glass Epoxy – 2 | 4.55 | $0^0$ |
| 28 | E-Glass Epoxy – 2 | 4.55 | $0^0$ |
| 29 | E-Glass Epoxy – 2 | 4.55 | $0^0$ |
| 30 | E-Glass Epoxy – 2 | 4.55 | $0^0$ |
| 31 | E-Glass Epoxy – 2 | 4.55 | $0^0$ |
| 32 | E-Glass Epoxy – 2 | 4.55 | $0^0$ |
| 33 | E-Glass Epoxy – 2 | 4.55 | $0^0$ |

2D Laminate Properties

| Title | Value |
|---|---|
| $E_x$ (MPa) | 4.61848E+04 |
| $E_y$ (MPa) | 2.16986E+04 |
| $G_{xy}$ (MPa) | 8.09538E+03 |
| $NU_{xy}$ | 2.52797E-01 |
| NUyx | 1.18769E-01 |
| $G_{xb}$ (MPa) | 4.61848E+04 |
| $G_{yb}$ (MPa) | 2.16986E+04 |
| $Gx_{yb}$ (MPa) | 8.09538E+03 |
| $NU_{xyb}$ | -2.52797E-01 |
| $NU_{yxb}$ | -1.18769E-01 |
| $CTE_x$ (mm/mm/C) | 4.54270E-06 |
| $CTE_y$ (mm/mm/C) | 2.66199E-06 |
| Density (g/mm3) | 2.06713E-03 |
| Thickness (mm) | 1.50150E+02 |

3D Laminate Properties

| Title | Value |
|---|---|
| $E_x$ (MPa) | 4.61848E+04 |
| $E_y$ (MPa) | 2.16986E+04 |
| $E_z$ (MPa) | 2.16986E+04 |
| $G_{xy}$ (MPa) | 8.09538E+03 |
| $G_{xz}$ (MPa) | 8.09538E+03 |
| $G_{yz}$ (MPa) | 7.91302E+03 |
| $NU_{xy}$ | 2.52797E-01 |
| $NU_{yx}$ | 1.18769E-01 |
| $NU_{xz}$ | 2.52797E-01 |
| $NU_{zx}$ | 1.18769E-01 |
| $NU_{yz}$ | 3.72876E-01 |
| $NU_{zy}$ | 3.72876E-01 |
| $CTE_x$ (mm/mm/C) | 4.54270E-06 |
| $CTE_y$ (mm/mm/C) | 2.66199E-06 |
| CTEz (mm/mm/C) | 2.66199E-06 |
| Density (g/mm3) | 2.06713E-03 |
| Thickness (mm) | 1.50150E+02 |

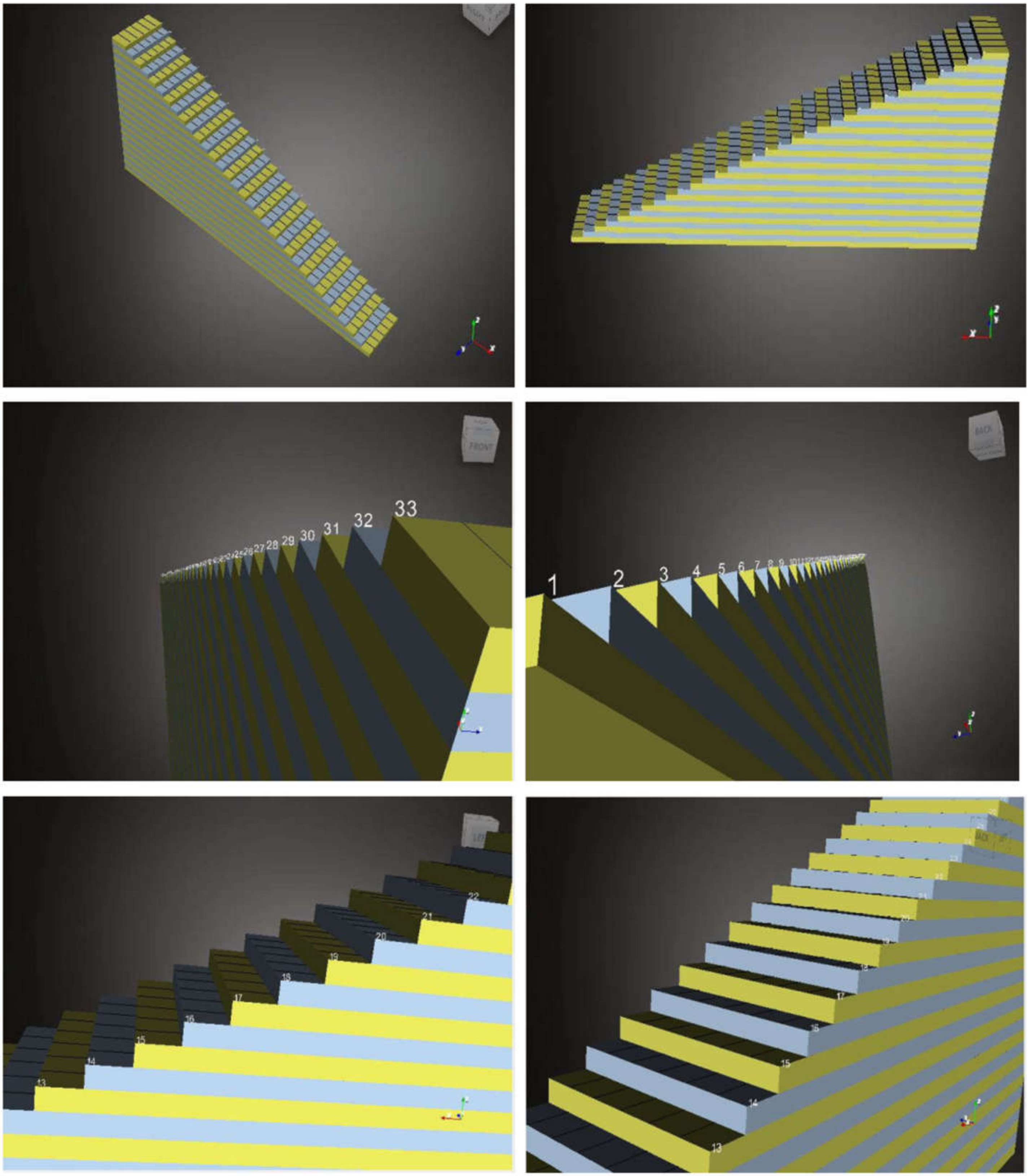


Figure 4.6. E-Glass Epoxy composite ply stacking sequence

## Appendix B

Vehicle traffic accident in Ethiopia

Table 1: Total number of accidents - severity

| YEAR | TOTAL NUMBER OF ACCIDENTS | | | | TOTAL |
|---|---|---|---|---|---|
| | LIGHT | HEAVY | FATAL | PROPERTY DAMAGE | |
| 2000/01 | 2,134 | 1,697 | 1,261 | 6,684 | 11,776 |
| 2001/02 | 2,196 | 1,712 | 1,327 | 7,188 | 12,423 |
| 2002/03 | 2,365 | 1,790 | 1,510 | 8,563 | 14,228 |
| 2003/04 | 2,705 | 2,072 | 1,630 | 10,569 | 16,976 |
| 2004/05 | 2,731 | 2,368 | 1,801 | 10,822 | 17,722 |

Table 2: Total number of accidents – Fatality by age group

| YEAR | NUMBER OF DEATHS | | | TOTAL |
|---|---|---|---|---|
| | YOUNG | MATURED | OLD | |
| 2000/01 | 934 | 472 | 154 | 1,560 |
| 2001/02 | 951 | 477 | 199 | 1,627 |
| 2002/03 | 1,124 | 487 | 203 | 1,814 |
| 2003/04 | 1,293 | 370 | 248 | 1,911 |
| 2004/05 | 1290 | 678 | 220 | 2,188 |

Table 3: Total number of accidents – Injured by age group

| YEAR | NUMBER OF PERSONS INJURED | | | TOTAL |
|---|---|---|---|---|
| | YOUNG | MATURED | OLD | |
| 2000/01 | 4,077 | 1,769 | 541 | 6,387 |
| 2001/02 | 4,309 | 1,750 | 543 | 6,602 |
| 2002/03 | 4,491 | 1,898 | 627 | 7,016 |
| 2003/04 | 4,625 | 2,372 | 880 | 7,877 |
| 2004/05 | 1,290 | 678 | 220 | 2,188 |

Source: Central Bureau of Federal Police commission

Table 3: Crashes by Collision and Vehicle Type (Getu S., Simon W, Mark J, August 2013)

| Traffic Accident Contributory Factors by type of crashes | | | | | | | | | | |
|---|---|---|---|---|---|---|---|---|---|---|
| No. | Description | | | | | | | | | |
| | Collision Types | | | | | Vehicle type | | | | |
| | Collision Types | Fatal Crashes | % | Injury Crashes | % | Vehicle type | Fatal Crashes | % | Injury Crashes | % |
| 1 | Head –on collisions | 604 | 4.98 | 608.98 | 4.48 | Cycle and Motorcycle | 451 | 3.71 | 1258 | 4.27 |
| 2 | Rear-end collisions | 333 | 2.74 | 335.74 | 4.16 | Automobile and Land Cruiser | 1204 | 9.92 | 5606 | 19.0 |
| 3 | Broadside collision | 284 | 2.34 | 286.34 | 2.85 | Commercial Vehicle | 5780 | 47.6 | 11124 | 37.7 |
| 4 | Sideswipe collision | 260 | 2.14 | 262.14 | 2.72 | Minibuses and Buses | 4191 | 34.5 | 10569 | 35.8 |
| 5 | Rollover | 2105 | 17.34 | 2122.34 | 17.17 | Earth Moving | 183 | 1.51 | 248 | 0.84 |
| 6 | Collision with pedestrians | 5894 | 48.44 | 5942.55 | 53.16 | Rail | 2 | 0.02 | 5 | 0.02 |
| 7 | Fall from vehicles | 1024 | 8.43 | 1032.43 | 6.46 | Animal Drawn Cart | 48 | 0.40 | 126 | 0.43 |
| 8 | Collision with animals | 609 | 5.02 | 614.02 | 4.23 | Others | 7o | 0.58 | 173 | 0.59 |
| 9 | Collision with parked vehicles | 219 | 1.8 | 220.8 | 1.49 | Unknown | 211 | 1.74 | 345 | 1.17 |
| 10 | Collision with road side objects | 370 | 3.05 | 373.05 | 1.43 | Total | 12140 | 100 | 29454 | 100 |
| 11 | With Train | 233 | 1.92 | 234.92 | 0.07 | | | | | |
| 12 | Others | 100 | 0.82 | 100.82 | 0.74 | | | | | |
| 13 | Unknown | 105 | 0.86 | 105.86 | 1.04 | | | | | |
| 14 | Total | 12140 | 100 | 12240 | 100 | | | | | |